BIOPOTENTIAL BASED ASSISTIVE DEVICE FOR HUMAN MACHINE INTERFACE

A THESIS

submitted by

S. SAI SURYA TEJA

in partial fulfilment of the requirements
for the award of the degree of

BACHELOR OF TECHNOLOGY
(Electrical Engineering)

and

MASTER OF TECHNOLOGY
(Biomedical Engineering)

DEPARTMENT OF ELECTRICAL ENGINEERING
DEPARTMENT OF APPLIED MECHANICS
INDIAN INSTITUTE OF TECHNOLOGY MADRAS

MAY 2015

I would like to dedicate this thesis to my loving parents

THESIS CERTIFICATE

This is to certify that the thesis titled **Biopotential based assistive device for human machine interface**, submitted by **Mr. S Sai Surya Teja**, Roll No. **EE10B119**, to the Indian Institute of Technology, Madras, for the award of the **Dual Degree** (Bachelor of Technology & Master of Technology), is a bona fide record of the research work done by him under our supervision. The contents of this thesis,in full or in parts, have not been submitted to any other Institute or University for the award of any degree or diploma.

Dr. M. Ramasubba Reddy
Research Guide
Professor
Dept. of Applied Mechanics
IIT Madras, 600036

Dr. Nitin Chandrachoodan
Research Guide
Associate Professor
Dept. of Electrical Engineering
IIT Madras, 600036

Place: Chennai

Date: 5th May 2015

ACKNOWLEDGEMENTS

I would like to express my gratitude to my project advisers, Dr. Nitin Chandrachoodan and Dr. M. Ramasubba Reddy for giving me this wonderful project. It is their guidance, support and encouragement that motivated me to work and come up with solutions to the problems I faced during the course of the project. The confidence I gained over the last year by working in this project has been tremendous and I would treasure the same.

I am deeply indebted to 'Open BCI' community for guiding me to design hardware and software for my project. I would also like to thank 'Texas Instruments' for their wonderful documentation and free samples without which it would have been difficult to start designing hardware for the project. I would like to thank my senior, Jobin for his valuable suggestions to overcome the difficulties that I faced during the course of my project. I thank IITMSAT team for giving me an opportunity to work in building a satellite which equipped me with all the skills required to complete my final year project.

I would like to thank all the members of Biomedical instrumentation lab for making this lab a fun place to work. Additionally, my special thanks to Sharat for being an awesome research partner and Ashwin for making me listen all sorts of melodious songs.

I take this opportunity to thank all my friends who provided the fun quotient to my campus life. Special thanks to Sandeep, Karthik, Kiran, GV, Raymond, Siva and Ramana for their support in every aspect and believing in me more than myself.

ABSTRACT

Since many years, the input from the human to the machine was managed through keystrokes in the keyboard, hand movements using a computer mouse, based on speech or gestures, etc. which requires fine motor control. An increasing number of people suffer from neuromuscular diseases that affect their capacity to communicate with the computer. Development of a user-friendly assistive device which can be controlled intuitively, without requiring extensive training to gain reliable control and aid these people in communicating with computer is quite helpful. Development of such a device needs careful design, to achieve good speed, accuracy and ease of use. Brain Computer interface (BCI) using Steady State visually evoked potentials (SSVEP) and eye tracker based on Electrooculogram (EOG) are chosen for this purpose. Aim of this project is to develop an in-house low cost bio-potential based assistive device.

The system must be portable and small enough to mount on a person as a wearable device. ADS1299 - a low noise, 8 channel, 24 bit analog front-end for biopotential measurements was chosen for this purpose. This mixed signal processor has instrumentation amplifiers (INAs), filters and analog to digital converters (ADCs) embedded in a single TQFP-64 package which serves the purpose of small size and portability. ATmega328p, a low power micro-controller is used to interface with ADS1299. 'Processing (language)' based applications are designed in PC to acquire and process the raw data from ADS1299 - ATmeag328p system.

The strength of (SSVEPs) have been observed to greatly depend on the stimulation source and paradigm. Orientation and size specific neurons have been discovered in the occipital cortex, which activate only when excited with specific

patterns. Different shapes have different orientation and size aspects that eventually lead to activation of different neuronal groups. In this project the potential for a novel shape switching based stimulation paradigm for SSVEP elicitation is investigated. Pattern reversal stimuli was found to elicit stronger SSVEP relative to single graphic stimuli. Results indicate that there might exist a subject dependent connection between the elicited SSVEP and choice of shapes for the stimulation paradigm. For SSVEP based BCI, the developed biopotential acquisition system is used to acquire 8 channel EEG at the occipital lobe. Visual stimulator to elicit SSVEP, software for signal processing and control are implemented in 'Processing (language)'. An online SSVEP based BCI system supporting four commands was successfully implemented with a decode speed of 1 command per 5 seconds. This thesis describes the data acquisition and processing software for an SSVEP based system. Other details are covered elsewhere.

An EOG based virtual keyboard is an another assistive device designed as a part of this project. A wearable dry electrode mask connected to the developed hardware is used to acquire 2 channel (vertical and horizontal) EOG signals. A virtual keyboard application with 26 alphabets, 10 digits and three special keys (backspace, enter, space) is design in 'Processing (language)'. The raw EOG data is processed and decoded in the background of the application. Left, right and blink gestures from the user eye are decoded into commands which helps the user to navigate left, right and select a character respectively on the virtual keyboard. An average typing speed of 1 char per 5 seconds was achieved using this system.

Contents

List of Tables

List of Figures

Nomenclature

Acronyms / Abbreviations

ADC Analog to Digital Convertor

BCI Brain Computer Interface

CCA Canonical Correlation Analysis

CMRR Common Mode Rejection Ratio

CRP Corneal Retinal Potential

CS Chip Select

DAQ Data Acquisition System

DIN Data In

DOUT Data Out

EEG Electroencephalogram

EMG Electromyogram

EOG Electrooculogram

ERD Event Related Desynchronization

ERP Event Related potentials

ERS Event Related Synchronization

HCI Human Computer Interface

IC Integrated circuit

IDE Integrated Development Environment

ITR Information Transfer Rate

KSPS Kilo Samples Per Second

MISO Master In Slave Out

MOSI Master Out Slave In

PC Personal Computer

PCB Printed Circuit Board

PSDA Power Spectral Density Analyzer

SCLK Serial Clock

SCP Slow Cortical Potential

SoC System On Chip

SPI Serial Peripheral Interface

SSVEP Steady State Visual Evoke Potential

TVEPs Transient Visual Evoke Potential

UART Universal Asynchronous Receiver transmitter

Chapter 1

Introduction

1.1 Motivation

With the advent of new technologies machines have become an important part of human life. There are many ways in which a healthy person interacts with these machines. In many cases, these interactions require fine motor control of hand. A significant number of individuals have several physical limitations, which limit them from accessing the advance communication and entertainment technology. These individuals often have motor neuron disabilities like cerebral palsy, spinal cord injury, amyotrophic lateral sclerosis, multiple sclerosis, muscular dystrophy, or traumatic brain injury.Communication between humans seems much simpler than the one that involve human machine interaction. Hence, it is very difficult for the patients to operate devices like keyboard, mouse, etc. Alternative computer input devices are now available in a variety of choices, to support special needs in communication. Several of these devices target the motor skills that are still available to the individuals. Tonguepoint system [3] is based on a pressure sensitive isometric joystick fixed firmly to mouthpiece, so that users will operate by tongue movement. Headmouse [4] will transform head movement into cursor movement on the screen. This is accomplished by a wireless optical sensor that tracks a small adhesive backed target on the user forehead or glasses. A lot of attention from the user is required to control the above devices. It can be quite strenuous. In cursor control applications, the method of signaling a mouse click is based on dwell times. These approaches can be very tricky for the user. Moreover, camera and processing can make the system more expensive. Very difficult to use for patients who doesn't have the fine motor control. In the past decades, several

people have widely reported the limitations of human computer interface (HCI) tools. However there was a tremendous progress in this field in recent years, there has been increasing interest in exploiting bio-electric signals such as EMG, EOG, EEG for the purpose of devising various type of HCI. Some of the other techniques like, automatic gesture recognition, analysis of facial expression, eye tracking, force sensing has gained more interest as potential modalities for HCI. Another approach is the usage of EEG waves originating in the brain. In this project we focused on two types of biopotential based assistive devices. One was the Brain Computer Interface (BCI) based on the Electroencephalogram (EEG) and the second one - an electroocculgram (EOG) based virtual keyboard.

1.2 Brain Computer Interface (BCI)

Ever since the discovery of the electrical characteristics of the brain by Dr. Hans Berger [5] , we have come a long way in deciphering, augmenting and interpreting the brain functioning. What was then considered to be a complex meaningless electrical (magnetic) signal has been unfolded into different characteristic components, which give significant insight into the state and operation of the brain. Besides diagnosis, it can be used as a non-traditional pathway for interaction with humans. The class of devices falling to the latter category of applications was collectively termed as Brain Computer Interface System, formally defined by Wolpaw et al at the First International Meeting on BCI Technology (2000) as a communication system that does not depend on the brains normal output pathways of peripheral nerves and muscles [6]. Interest in the domain has spiked because potential applications of such systems [7] [8]. Also, recent developments in Neuroscience, Signal Processing and Machine Learning has contributed to subsequent improvement in system feasibility and implementation.

A brain computer interface (BCI) system primarily involves harness of the electromagnetic signals acquired from the brain and/or neural system. Different differ-

entiable types of EEG signal is available as electrode output on placement of the same. The dominant type is primarily governed by the spatial location of the electrodes and the state of the brain at any temporal instant. The spatial-temporal nature of the EEG signal is decisive enough to be used for a BCI system. EEG signals can be broadly classified as follows:

- Event Related Potentials [ERP] : P300, SSVEP
- Oscillatory Brain Activity : Delta [1-4 Hz], Theta [4-8 Hz], Alpha & Mu [8-13 Hz], Beta [13-25 Hz], Gamma [25-40 Hz]
- Slow Cortical Potentials
- Neuronal Ensemble Activities
- Sensorimotor Cortex Rhythms

Of these, the ERPs, SCPs and sensorimotor cortex rhythms are widely researched for use in BCI systems. Broadly speaking, BCI systems are classified based on the type of activation signal used for interface. Slow Cortical Potentials abbreviated as SCP are slowly varying potentials found on the scalp ($0.5 - 10$s). These signals are manipulated based on user intention. Positive SCPs indicate reduced low cortical activation rates whilst negative SCPs are indicative of increased cortical activation due to increased muscle movement or other activities yielding increased cortical activation. Birbaumer [9] et al has shown that people can learn to control these potentials and hence be used to interface BCI systems. The primal drawback of this method is the need for intensive training of the order of days or months.

The P300 wave discovered by Sutton [10] is known to be produced from the human scalp when an unlikely event occurs between events of high probability. The signal is known to be produced at a 300 ms delay from the onset of the stimulus, hence the nomenclature of the signal. On using the P300 as a spelling device, for which it is widely researched on, characters are flashed on the screen. User is asked to count the number of times the character of his\her choice is flashed. By doing so, a

P300 is elicited from the user scalp each time the character of choice is projected. To account for greater accuracy and reliability multiple counts of elicited P300 have to be used to characterize user selection. Characters can be either projected single element vice or row-column vice depending on the application requirements such as number of selections to be made etc. One may also use P300 for control tasks as shown by Finkea [11] and navigation as shown by Citi (mouse movement) [12].

Steady State Visual Evoked Potentials, abbreviated as SSVEP signals are EEG signals elicited in response to a visual stimulus flickering at constant frequency in the range of 5-50 Hz [13]. By repeated visual stimulation at a frequency greater than 5Hz, the quasi sinusoidal Transient Visual Evoked Potential (TVEP) is merged to yield a near sinusoidal SSVEP resonant at the stimulation fundamental frequency and it's harmonics [14].

Originating predominantly from the occipital parietal region [15], the near sinusoidal SSVEPs are frequency and phase locked to the flicker frequency of the visual stimulus. SSVEP based BCIs uses several flashing light sources that flash at a predetermined frequency. The user focuses on one of the sources of choice, which is the understood by studying the SSVEP signals elicited in occipital and parietal regions of the brain. The frequency of the elicited SSVEP signal is observed to be the same as that of the generating source, which is used as a cue to identify source of interest. Classification can be done by using native techniques as PSDA, which analyzes the power content in the frequency of interest. Recently, the use of multiple EEG channels for effective SSVEP detection has been found give improved performance [16]. The Canonical Correlation Analysis (CCA), proposed by Lin et al [17] and the Minimum Energy Channels [16], proposed by Friman et al, are variants of optimal channelization to improve performance. Based on the classification result, some action is performed. SSVEP based BCIs find applications in navigation [18] etc. Gao et al [19] experimented by using 48 different classes. Bakardijan et al [20] demonstrated that maximum SSVEP response is

obtained between 5.6 Hz and 15.3 Hz from 5-48 Hz range. Allison [21] and Zhang [22] have shown that selective attention onto a target alone is sufficient to obtain an accurate SSVEP signal.

As shown by Pfurtscheller [23] and Neuper [24], ERD (Event Related Desynchronization) signals are generated in the sensory motor cortex in the event of motor cortex related activity. 2 seconds before the actual movement of the limbs, there is a relative decrease in power in the upper alpha band and lower beta band on the contra lateral hemisphere. Eventually it becomes bilaterally symmetrical just before movement execution. Like ERD, ERS (Event Related Synchronization) signals can also be used to detect an event related to motor activity. It may occur at the termination phase of the movement or simultaneous to the ERD but with the difference being in the spatial point of origin.

BCI applications include spellers, environmental control, wheelchair control, neuromotor prosthesis, gaming and virtual reality. The greatest challenges in development of a BCI system are the implementation of asynchronous nature in a BCI system and implementation of a BCI without training [25]. Performance of a BCI system can be numerically analyzed using it's classification accuracy and the information transfer rate (ITR). The ITR is represented either in bits\selection or bits\min [6] keeping in convention of a standard communication system. ITR depends on time segment length (buffer length) used and the algorithm processing speed.

Whilst larger time segments yield better accuracy, they make the system less feasible for online implementations because of slower response. Hence, a tradeoff needs to be set for feasible accuracy at smallest buffer size possible for effective online implementations.

1.3 EOG based Human Computer Interface

Electrooculograms (EOGs) are strong bio-potentials induced by eye movements. The metabolically active retinal epithelium generates the Corneal Retinal Potential (CRP), which imparts the eyeball it's dipole characteristics [26]. Using bi-channel acquisition with electrodes aligned along the horizontal and vertical axes, signals pertaining to the eyeball movement can be acquired. Useful EOG features are generally observed in the 10-100 µV magnitude range and 0- 10 Hz frequency range [26]. EOGs being essentially eye movement dependent can be manipulated by a human, which offers a way for an effective human-computer interaction. Potential applications of EOG include context recognition systems [27] and assistive technology such as wheelchairs [28] [29], alarm systems [26] etc. Despite it's relatively high magnitudes, EOG signals are still susceptible to non-deterministic variations since they are governed by numerous parameters such as eye blinks, electrode placement, head movement, luminance etc., which need not be constant across subjects and sessions. The ocular muscles work individually or in synchrony to provide the overall motion of the eyeballs thereby positioning the eye in the direction of vision. These movements can be broadly classified into four categories:

- Saccades : These movements occur in the eye which are associated with the normal functioning such as reading, gazing, etc. These movements are mostly involuntary but can be voluntary sometimes.
- Vestibulo-ocular movements : These movements help an individual to keep an object under the circle of vision even while the head is moving.
- Vergence movements : Unlike other movements, these movements function independently for each eye such that the perception of depth and distance can be achieved by superimposing the two images in the brain.
- Smooth pursuit movements : These are voluntary movements which are very

slow in nature.

Over the last decade researchers all over the world developed different EOG based assistive devices.

- Wijesoma et al. (2005) [30] developed initial model of a robotic wheelchair system based on electrooculography. They used MP150 Biopac system to acquire EOG signals and MATLAB for processing.
- Arslan Qamar Malik, and Jehanzeb Ahmad (2007) [31] designed and developed an EOG based mouse control device. They used INA126P, OPA277, ADS7800 to acquire EOG signals and then interface with computer through parallel ports.
- Manuel Merino et al. (2010) [32] developed a system to detect eye movement based on the EOG signal. They used Ag/AgCl sensors and BCI2000 and the amplifier g.USB amp for EOG acquisition.
- Usakli et al. (2010) [33] developed and realized a virtual keyboard that allowed the user to write messages and to communicate other needs based on EOG signals. 5 Ag/AgCl electrodes are used for EOG acquisition. They used LT1167, LMC6001, MAX281, PIC12F675, PC817 in their acquisition system design.
- Patterson Casmir D'Mello, Sandra D'Souza (2012) [34] developed a LabVIEW based EOG classification system. Ag/AgCl electrodes were used for EOG signal acquisition. M Series USB-6221 was used as a data acquisition interface.
- Divya Swami et al. (2012) [35] designed an EOG based typing system. A gUSB amplifier was used in filtering, amplification and analogue to digital conversion of EOG signals.

Though the above systems had a good performance, they lack reusability and wearability because of the electrode type (wet) and the bulky electronics. These

systems has to be improvised to wearable devices so that any disabled person can use them with ease. Moreover, the system should support dry electrodes for re-usability. Thus, a wearable device has been designed as a part of this project. Details of the implementation is explained in chapter 4.

Chapter 2

Biopotential Acquisition System

2.1 Introduction

Unlike other biopotential signals, EEG signals are in the order of 100 μV. The instrument need to have high common mode rejection ratio - CMRR (>100 dB) to seperate EEG from common mode signals. Ideally, instrumentation amplifiers with high CMRR and high gain along with analog filters (low pass and high pass filters) are used to implement the acquisition system for acquiring EEG signals. Gain of the amplifier must be adjusted so that output voltage lies in the dynamic range of analog to digital convertor (ADC). Finally, the digitized values are transferred to a computing device like PC or any standalone micro-processor system for storage and further processing. In most of the cases, a software application must be provided on the computing side so that the user can use the device with ease.

2.2 Market survey

There are many non-invasive consumer BCIs available in the market. Some of them are listed in table 2.1. These BCI kits are designed to acquire EEG signals supporting different number of electrodes based on the purpose. Though the internal hardwares of these kits can acquire any biopotential signals, structural design make them incapable of acquiring signals like EOG. Some of them are used for gaming while some of them to help in BCI research, etc. These kits can also be used as assistive devices with a custom made software. But the cost is too high (per number of channels) for a developer or consumer to bear.

Device	Price (in $)	Number of Electrodes	Sensors Interpretation
iFocusBand	310	1	8 mental states, facial tension, eye movement and quiet eye
Mindwave	99.95	1	2 mental states
Mindflex	50	1	1 mental states
Emitov EPOC	299	14	3 mental states, 13 conscious thoughts, head movements (sensed by gyro)
Star Wars Force Trainer	45	1	1 mental state
Mindset	199	1	2 mental states
Neural Impulse Actuator	90	3	2 brain waves (Alpha & Beta), facial muscle and eye movements
XWave headset	90	1	8 EEG bands
MyndPlay BrainBand	158	1	8 EEG bands

Table 2.1: Commercial non-invasive BCIs[1]

Apart from the mentioned BCI kits, general purpose data acquisition (DAQ) systems available for medical applications are very costly . Here are some of the DAQ available in the market.

1. BIOPAC MP36RWSW : Supports 4 isolated channels with maximum sampling speed of 100k samples/sec with 24 bit resolution for input ranging 4 V p-p. Cost : $ 8400

2. BIOPAC MP150WSW : Supports 16 channels with maximum sampling speed of 200k samples/sec with 16 bit resolution for input range 10 V p-p. Cost : $ 8100

3. Digital EEG KT88-2400 : Supports 19 EEG, 1 ECG, 1 EMG, 2 EOG and 1 channel for breath. Cost : $2108

4. Digital Electrocardiograph : Supports 12 lead ECG. Portable system. Cost : $254.

Addressing these issues, this project also aims at designing a low cost ($ 80 approx.

excluding electrodes cost) 8 channel (differential / single end) biomedical data acquisition setup with compact (wearable) size and wireless features.

2.3 Analog Front End

With the advancement in the semiconductor technology, system on chips (SoCs) have become popular over the past few decades. In the past, a biopotential acquisition system includes input protection circuit, instrumentation amplifiers, analog filters made of operational amplifiers, analog to digital converters (ADCs) and a microprocessor as individual blocks. Such a design has large form factor and consume large power. Moreover, the designer has to be very careful while designing the PCB layout and the system has to be completely shielded to reduce the noise. Hence, it is very difficult to design a precise, low power and a wearable biopotential acquisition system with the above set of components.

2.3.1 ADS1299

To overcome the above limitations we opted ADS1299, a SoC developed by Texas Instruments as the analog front end IC which replaces all the conventional ICs such as instrumentation amplifiers, operational amplifiers and ADC. ADS1299 is specifically meant to acquire EEG signals. Nevertheless, it can acquire any other biopotential signals. Some of the key features which makes ADS1299 ideal to include in the system are:

- It supports 8 single-end / differential analog input channels. Each channel has a 24 bit $\Delta\Sigma$ ADC with a maximum data rate of 16 KSPS and consumes 5 mW / channel. Internal reference of ADC can be programmed to 4.5 V.
- It has a very low input referred noise of 1 μV p-p and a CMRR of 110 dB.
- Gain of instrumentation amplifiers can be programmed to 1,2, 4, 6, 8, 12, 24.

- Supports serial peripheral interface (SPI) which is most common in many micro-controllers. Thus, it can be configured by any micro-controller. Moreover, many ADS1299 devices can be cascaded to design a high channel DAQ system in a daisy - chain configuration using the same SPI bus.
- Supports internal lead-off detection circuit based on current source or sink.

Functional block diagram of ADS1299 is shown in fig. 2.1.

2.3.2 ADS1299 control and status registers

All the important registers of ADS1299 can be grouped into three categories. They are described below.

2.3.2.1 Global Settings

This category includes three configuration registers viz. CONFIG1, CONFIG2, CONFIG3 and one lead-off control register viz.LOFF . These settings are applied to all the input channels of ADS1299. CONFIG1 is used to configure daisy chain, clock source (external / internal) and output data rate. CONFIG2 is used to configure amplitude and frequency of internal test signal. Internal test signal helps the user to test the functionality of ADS1299. CONFIG3 is used to configure bias reference signal (internal / external). As seen from fig 2.1, bias reference is a part of right leg driven circuit which improves CMRR of the system. LOFF is used to configure the lead off comparator threshold settings , lead off current magnitude and lead off frequency.

2.3.2.2 Channel Specific Settings

This category includes 13 registers viz. CHnSET (n = 1,2,..8), BIAS_SENSP, BIAS_SENSN, LOFF_SENSP, LOFF_SENSN, LOFF_FLIP. CHnSET is used to change the INA gain, select reference bias channel and disable or enable the channel. LOFF_SENSP, LOFF_SENSN selects the positive and negative side

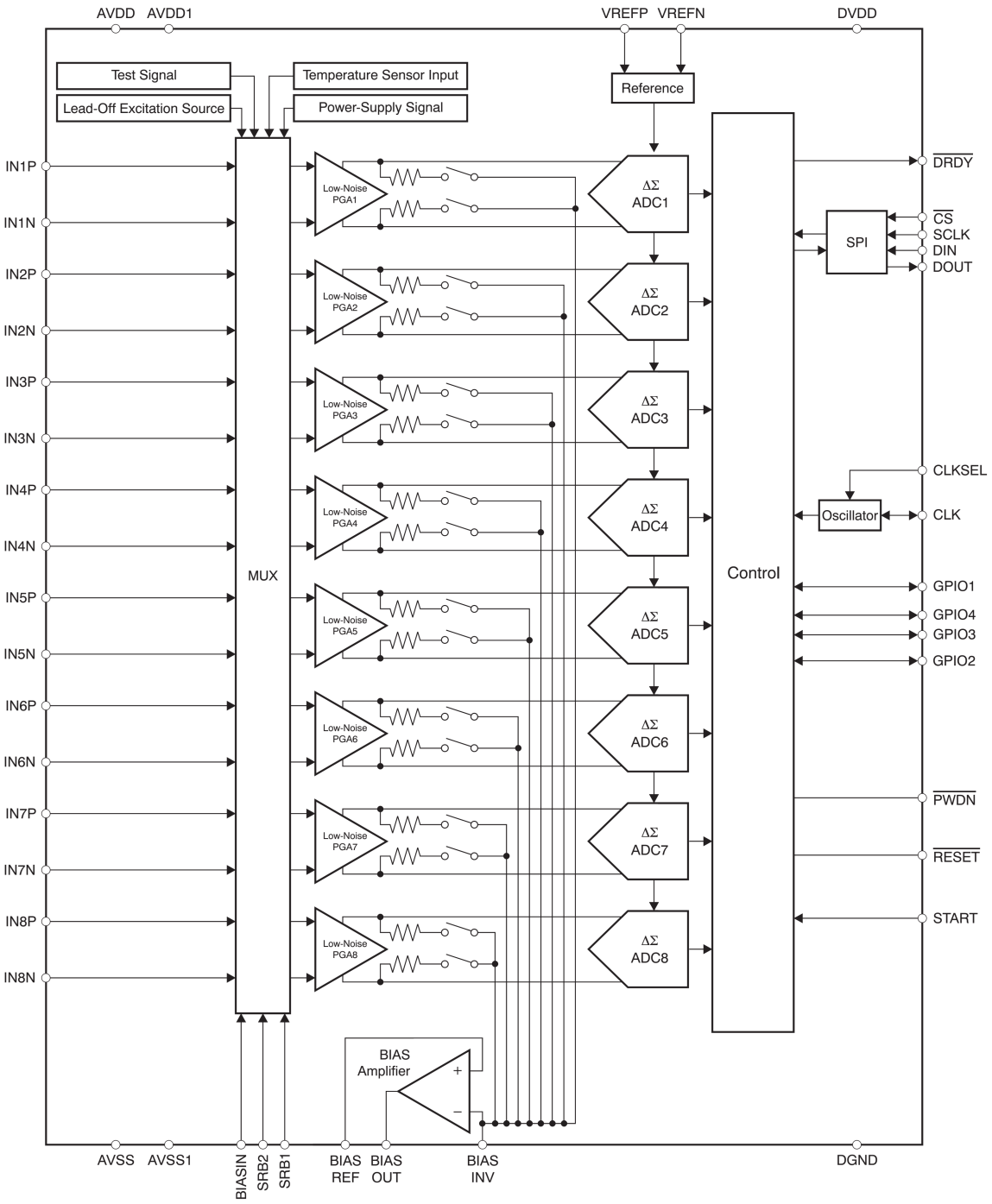

Figure 2.1: ADS1299 functional Block Diagram[2]

respectively from each channel for lead-off detection. LOFF_FLIP controls the current direction for lead-off derivation.

2.3.2.3 Lead-off status registers

This category includes LOFF_STATP and LOFF_STATN registers which stores whether the positive and negative electrodes on each channel is on or off respectively.

2.3.3 Theory of operation

Any micro-controller which supports serial peripheral interface (SPI) has four signals: $\overline{CS}$(chip-select), SCLK (serial clock), MOSI (master out slave in), MISO (master in slave out). Using these signals a micro-controller reads conversion data, reads and writes registers, and controls ADS1299 operation. Apart from these four signals, ADS1299 has $\overline{DRDY}$ signal asserts when the data conversion is complete by turning logic low. This acts as an indication for the micro-controller to read the digitized data from ADS1299. In this interface micro-controller acts as the master and ADS1299 acts as a slave. Master asserts $\overline{CS}$ to logic low to enable the slave. This signal has to remain low for the entire serial communication duration. SCLK is provided by the master which shifts in commands and shifts out data from ADS1299 for every rising / falling edge. MISO and MOSI are data lines though which data is transmitted. ADS1299 latches data on MOSI (DIN) on every SCLK falling edge where as data on MISO (DOUT) are shifted out on every SCLK rising edge. Fig 2.2 shows the ADS1299 data output protocol.

Specific op-code commands need to be used to control and configure ADS1299 operation. These can be categorized into three types viz.

1. System commands

2. Data read commands

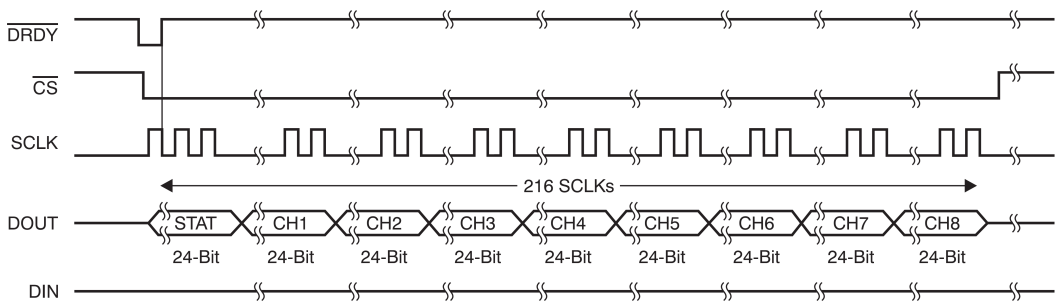

Figure 2.2: ADS1299 data output protocol [2]

3. Register read commands.

System commands include WAKEUP (op-code : 02h) , STANDBY (04h), RESET (06h), START (08h), STOP(0Ah). These commands control the state of ADS1299. WAKEUP is used to wake from stand by mode. STANDBY is to enter low power mode. RESET will reset the system and configures all the registers to default values. START will trigger the ADC conversion. An alternate of this command is to assert START pin of ADS1299 to logic high. START pin must be held low when using START op-code command. STOP will halt the conversion.

Data read commands include RDATAC (10h), SDATAC (11h), RDATA (12h). These commands control the data flow from ADS1299. RDATAC will allow the micro-controller to read data continuously for every trigger from $\overline{DRDY}$. SDATAC will stop the continuous read mode. RDATA configures ADS1299 to transfer data only on command and not continuously.

Unlike system and data read commands, register read commands are two op-code commands. RREG and WREG are used to read and write 'n' registers starting from the address mentioned in the first op-code where 'n' is mentioned in the second op-code. In our system, we use WREG to configure all control registers of ADS1299 and later send RDATC to receive data continuously.

2.4 BioDaq v01- Schematics

As a first prototype of biopotential data acquisition system, we designed BioDaq v01 as an arduino shield. An Arduino uno is used as the micro-controller board to interface with ADS1299 housing at the center of BioDaq v01. Though BioDaqv01 is an arduino shield, it is designed as a genric board which can interface with any other micro-controller. See appendix A for the detail list of bill of materials. Few important components which are essential in BioDaq v01 are as follows :

- ADS1299 (24 bit, 8 channel analog front end IC by TI)
- TPS60403 (charge pump inverter)
- TPS73225 (2.5V Regulator)
- TPS72325 (-2.5V Regulator)
- TPS70933 (3.3V Regulator)
- TXB0108 (Used for logic translator). Useful when trying to interface with any other micro-controller with different logic levels.

As shown in fig 2.3, ADS1299 requires three supplies viz,. DVDD - digital supply which used for digital circuitry like internal SPI module, AVDD - positive analog supply, AVSS - negative analog supply. One of the standard procedure in acquiring any biopotentials is to use anti-aliasing filters to remove high frequency signals so as to avoid aliasing effects after sampling. We used first order anti-aliasing filter using 5K resistor and 4.7nF capacitor before every electrode. This can be seen in fig 2.3.

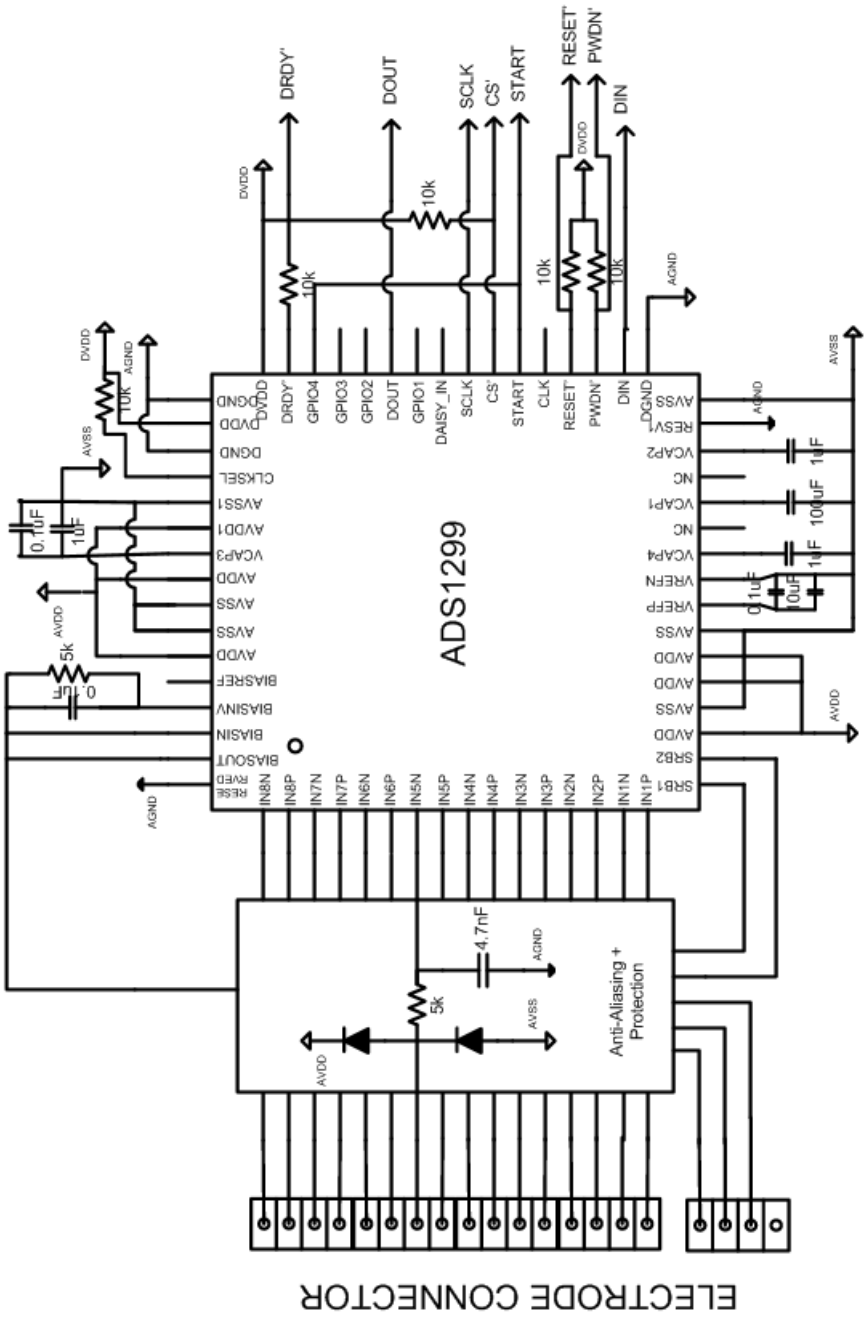

Figure 2.3: Schematics of ADS1299

The generic board that we have designed can accept voltages supply greater than 3.3V supply and convert to DVDD, AVDD and AVSS. fig 2.4 shows the power supply ICs which we have used to achieve this. Since, the generic board is designed to interface with any micro controller (μC), we have used a voltage level shifter , TXB108 for a proper SPI communication between ADS1299 and μC.

2.5 BioDaq v01 - PCB layout

Figure 2.5 shows the top and bottom layers of the BioDaq v01 mother board. ADS1299 is soldered on a separate IC base which is then mounted on the motherboard.This way, even if the motherboard is spoiled for some reasons, ADS1299 can be unplugged from it and can be plugged on to a new board. It is also helpful when migrating to newer designs in the development stages. Since we are dealing with sensitive analog signals, certain PCB guidelines are followed. Some of them are:

- The ADS1299 power supplies includes AVDD, AVDD1, and DVDD. As both the AVDD and AVDD1 are used in analog operation of ADS1299 they should be as quiet as possible. AVDD1 is known to have transients at f_{CLK} (clock source for ADS1299) as it supplies to the charge pump block . Hence, we need to separate the power planes of AVDD1 and AVSS1 from AVDD and AVSS. They should be star connected with the junction node near to the supply.

- To filter AC signal noise in the power supply 1 μF and a 0.1 μF solid ceramic capacitors are used for each supply of ADS1299.

- Digital circuits like micro-controllers on the layout must be placed with at most care so that the return currents on those devices should not cross the analog return path of ADS1299. Since the BioDaq v01 is an arduino shield, there is no need to worry about this issue.

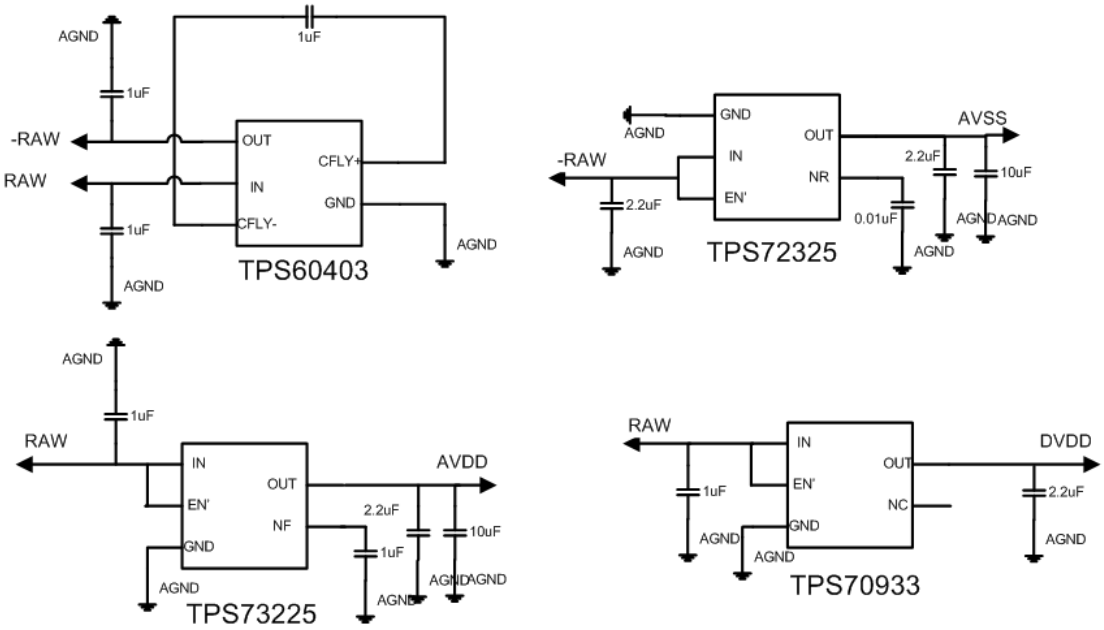

Figure 2.4: Power supply Schematics

- Since the analog inputs have very high input impedance, they are extremely sensitive to extraneous noise. Hence, direct connections avoiding any stray wiring capacitance is ensures at analog input pins. It is recommended to treat AVSS pin as a sensitive analog signal and connect directly to the supply ground with proper shielding.

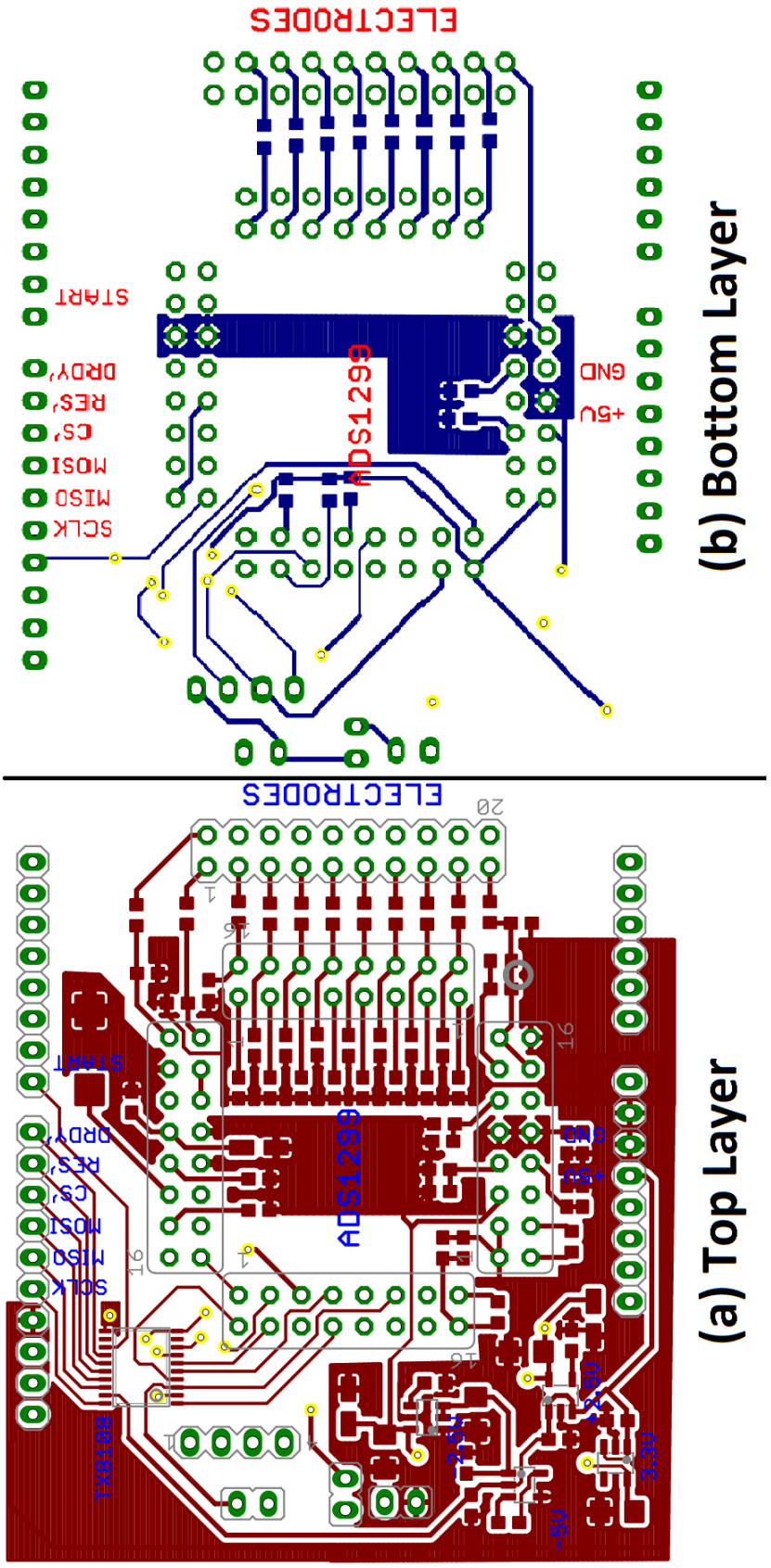

Figure 2.5: BioDaq v01 PCB Layout

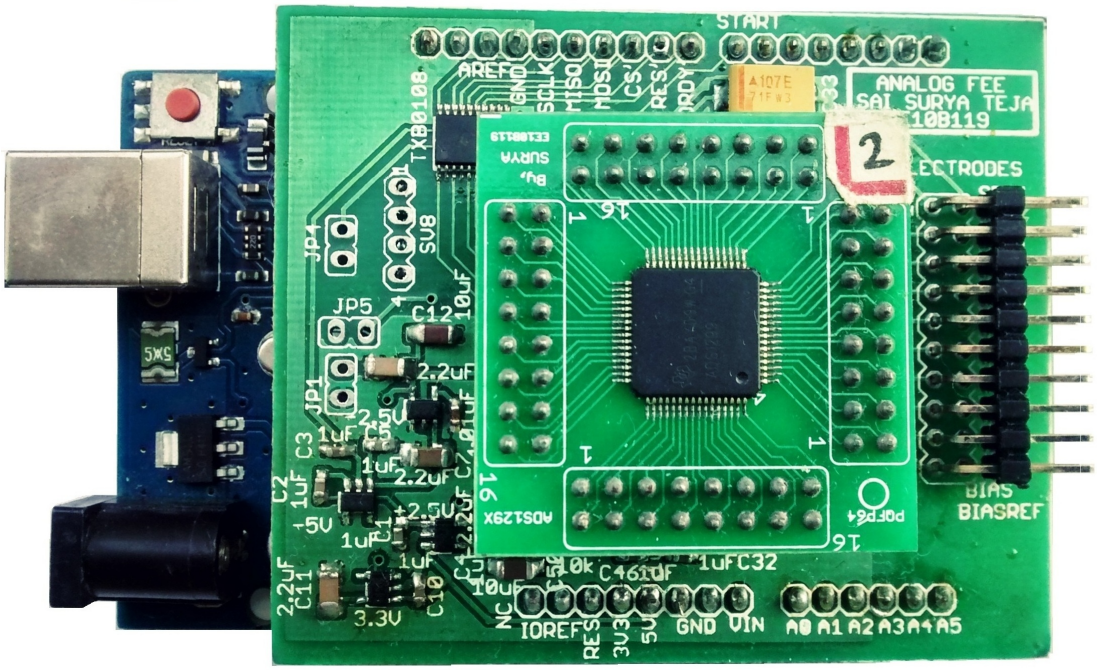

Figure 2.6: BioDaq v01 mounted on arduino UNO

2.6 Final hardware Setup

Figure 2.6 shows bioDaq v01 mounted on arduino uno. Arduino is connected to PC via serial universal asynchronous receiver transmitter (UART) bus. This system has provision to connect 8 electrodes (single-end / differential) , a bias signal (used in single-end mode), BIASREF and BIAS_ELECTRODE. The latter two are used in right leg driven circuit which improves the CMRR of the system.

2.7 Initial Hardware Tests

2.7.1 Testing SPI link

As discussed in section 2.3.3, ADS1299 operation is controlled by SPI op-code commands. After a system reset, all the registers of ADS1299 are automatically set to default values. In order to test the working condition of SPI link between ADS1299 and arduino, op-code value corresponding to RREG is sent from arduino to ADS1299 to read all the default register values. fig 2.7 (a) shows the default

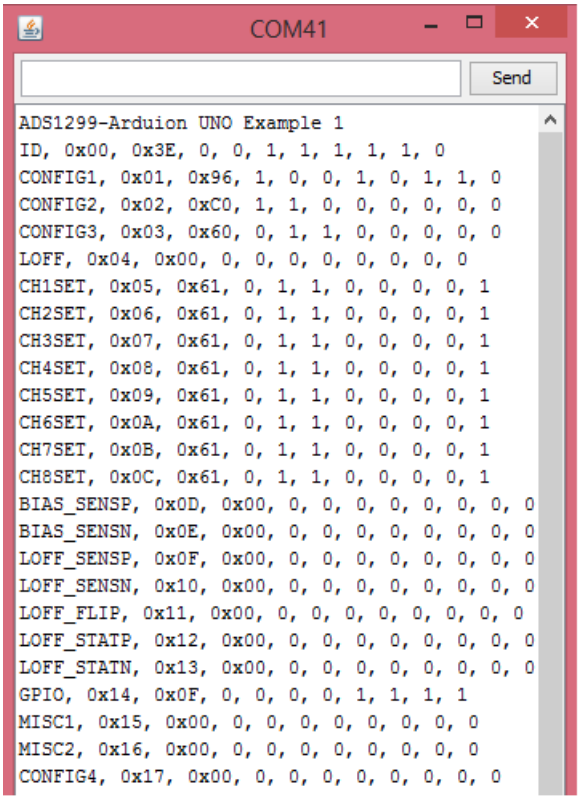

ADDRESS	REGISTER	RESET VALUE (Hex)
Device Settings (Read-Only Registers)		
00h	ID	00
Global Settings Across Channels		
01h	CONFIG1	96
02h	CONFIG2	C0
03h	CONFIG3	60
04h	LOFF	00
Channel-Specific Settings		
05h	CH1SET	61
06h	CH2SET	61
07h	CH3SET	61
08h	CH4SET	61
09h	CH5SET	61
0Ah	CH6SET	61
0Bh	CH7SET	61
0Ch	CH8SET	61
0Dh	BIAS_SENSP	00
0Eh	BIAS_SENSN	00
0Fh	LOFF_SENSP	00
10h	LOFF_SENSN	00
11h	LOFF_FLIP	00
Lead-Off Status Registers (Read-Only Register		
12h	LOFF_STATP	00
13h	LOFF_STATN	00
GPIO and OTHER Registers		
14h	GPIO	0F
15h	MISC1	00
16h	MISC2	00
17h	CONFIG4	00

Figure 2.7: Default register values of ADS1299

register values read from bioDaq v01 on a serial terminal. Each line on the serial terminal has register name, register address, register value (hex), register value (binary) in the respective order. Figure 2.7 (b) is to compare default register values described in the data sheet of ADS1299. Every transaction between ADS1299 and arduino is carried over SPI bus. This test verifies the working condition of micro-controller and ADS1299 interface.

2.7.2 Input Referred noise

Input referred noise is the default noise present int the system even when the inputs are shorted to the ground. Since, the designed instrument is mean to

Input channel no:	Input referred noise (μVrms)
1	0.1622
2	0.2025
3	0.1008
4	0.0965
5	0.175
6	0.0957
7	0.0996
8	0.1202

Table 2.2: Input referred noise

acquire EEG signals which are of 100uV magnitude, input referred noise must be very low. According to the data sheet of ADS1299, input referred noise at 250 Hz data rate is around 0.14 uV. We tested the designed hardware to check whether the input referred noise matches the data sheet value. RDATAC op-code command is used to acquire data continuously from ADS1299. Table 2.2 shows our observation table for input referred noise for all the 8 channels with all inputs connected to ground. The data is acquired by applying 50Hz digital notch filter and second order bandpass butter worth filter [0.1 - 65Hz]. On an average, the input referred noise is close to the value mentioned in the data sheet. This shows the PCB layout doesn't induce any extraneous noise.

2.7.3 Internal Test pulse of ADS1299

As seen from fig 2.1, ADS1299 has a provision to generate internal test pulse.To test the configuration settings of ADS1299, we program CONFIG2 register in ADS1299 to generate internal test pulse as discussed in section 2.3.2. Digitized data which is acquired over SPI bus is transferred to PC over serial UART bus. An application implemented in 'Processing (language)' receives the data from the COM port (to which Arduino is connected) and displays the waveform on the Open BCI (open source platform for BCI study) developed GUI. Figure 2.8 shows the test pulse acquired from bioDaq v01.

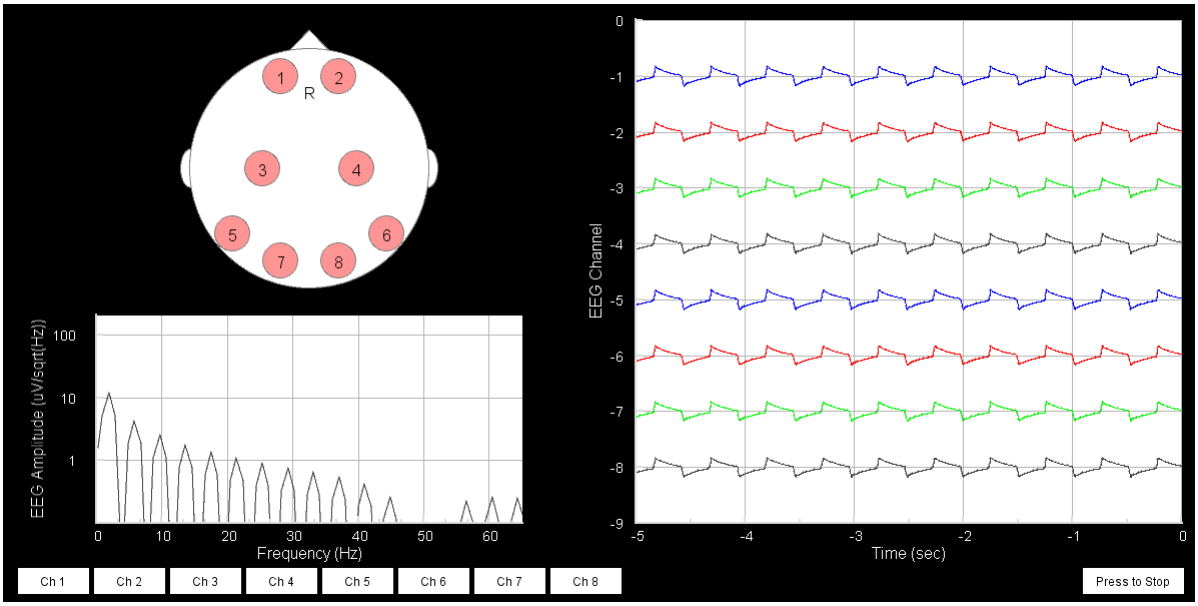

Figure 2.8: Test pulse generated from bioDaq v01 shown on Open BCI developed GUI

2.8 Design of BioDaq v02

Though the BioDaq v01 serves the purpose of low cost, low power biopotential data acquisition system, it lacks wireless feature and has a poor form factor which cannot be used as a wearable device. Taking this into consideration, BioDaq v02 is designed with a small form factor of size 6 x 4 sq-cm which can be used as a wearable device. Unlike bioDaq v01, version 02 doesn't use arduino uno. Instead, ATmega328P-AU is directly used on the PCB along with ADS1299. However arduino opti bootloader is uploaded into ATmega328p to make the system compatible with software used for bioDaq v01. It has a provision to connect a bluetooth module to make the system wireless and a provision for FTDI to program via UART bus. A detail analysis on the selection of bluetooth for a particular data acquisition system is discussed in Appendix B. We used HC05 as the bluetooth device in BioDaq v02. Bill of materials required for BioDaq v02 are mentioned in appendix A. Schematics of BioDaq v02 is very similar to BioDaq v01 expect for ATmega328P -AU replacing arduino uno. Figure 2.9 shows the top and bottom layout of bioDaq v02. Figure 2.10 shows bioDaq v02 packed in a tic-tac box along with a Nokia battery (800 mAh). It has a provision to switch on/off the device

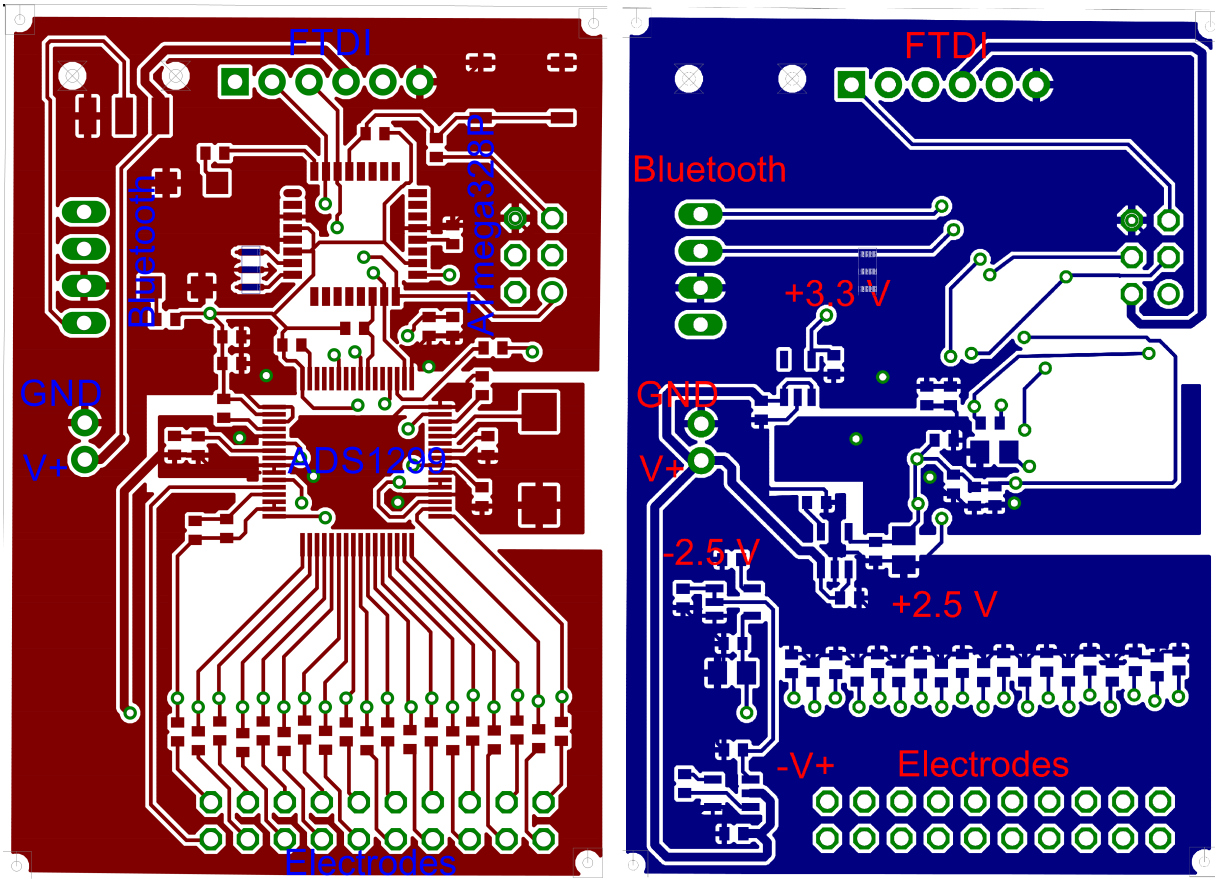

Figure 2.9: BioDaq v02 PCB layout

and a power jack to charge the battery. Any Nokia charger will serve the purpose.

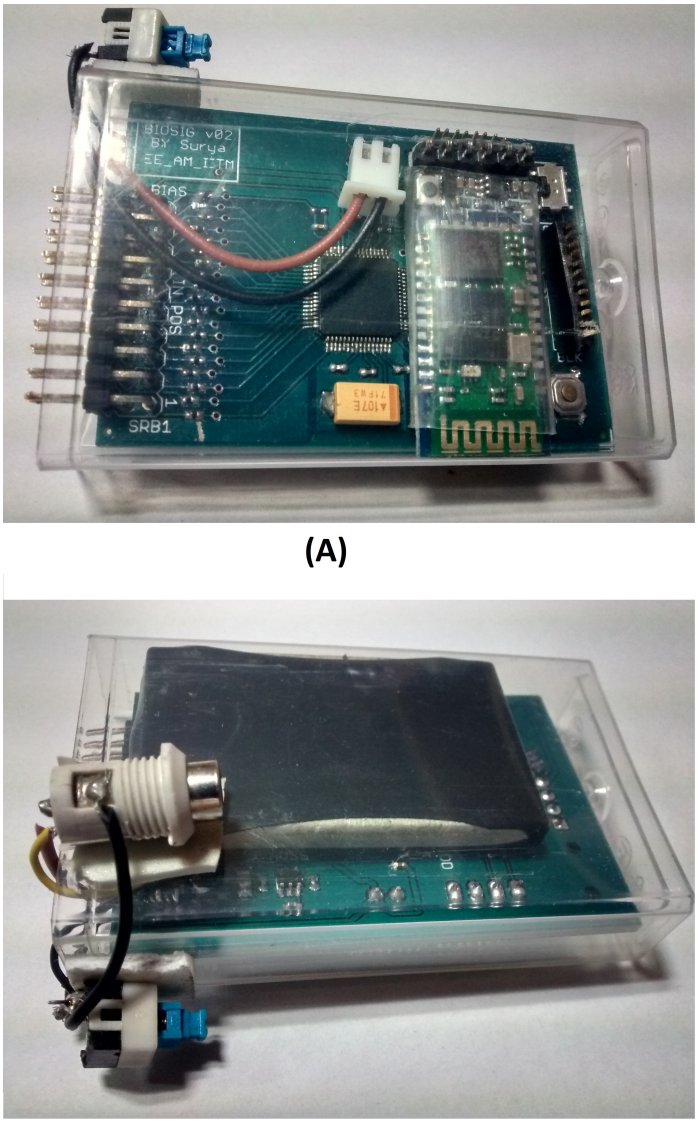

Figure 2.10: BioDaq v02 assembled in a tic-tac box. (A) Front view, (B) Back view

Chapter 3

SSVEP Based BCI system

BCI systems working based on SSVEP signals are known to produce high ITR and accuracy with minimal training [28]. Also, the fact there is significant ease of operability and minimum uncertainty further motivates the use of SSVEP signals for our work. Despite these facts, a full fledged implementation of such a system remains constrained to optimal conditions in a lab environment. Recently, the use of multiple EEG channels for effective SSVEP detection has been found give improved performance. Unlike other BCIs, SSVEP based BCI does not require any subject training. P300 based BCI also doesn't require training but the accuracy decreases after a certain time of usage whereas it is not the case with SSVEP based BCI. Figure 3.1 shows a block diagram of SSVEP based BCI system.

This chapter includes complete details of SSVEP based online BCI system and its implementation. The work mentioned in this chapter is a collaborative work with Mr.Sharat S. Embrandiri, an M.S student in Applied Mechanics, IIT Madras. I was involved in developing data acquisition system to acquire EEG and software for visual stimulator. Mr. Sharat was involved in developing novel algorithms to increase the classification speed and accuracy of SSVEP based BCI system. Apart from this, he also ideated the experiment to understand the effects of different shape stimuli on SSVEP strength 1 which is expalined in detail in this chapter.

3.1 BCI System functional segmentation

In general, the system can be segmented into different functional units as shown in 2.1. Initially, visual stimulus is provided to the user via a monitor or an LED grid array. The signals of interest are extracted using electrodes placed on the scalp

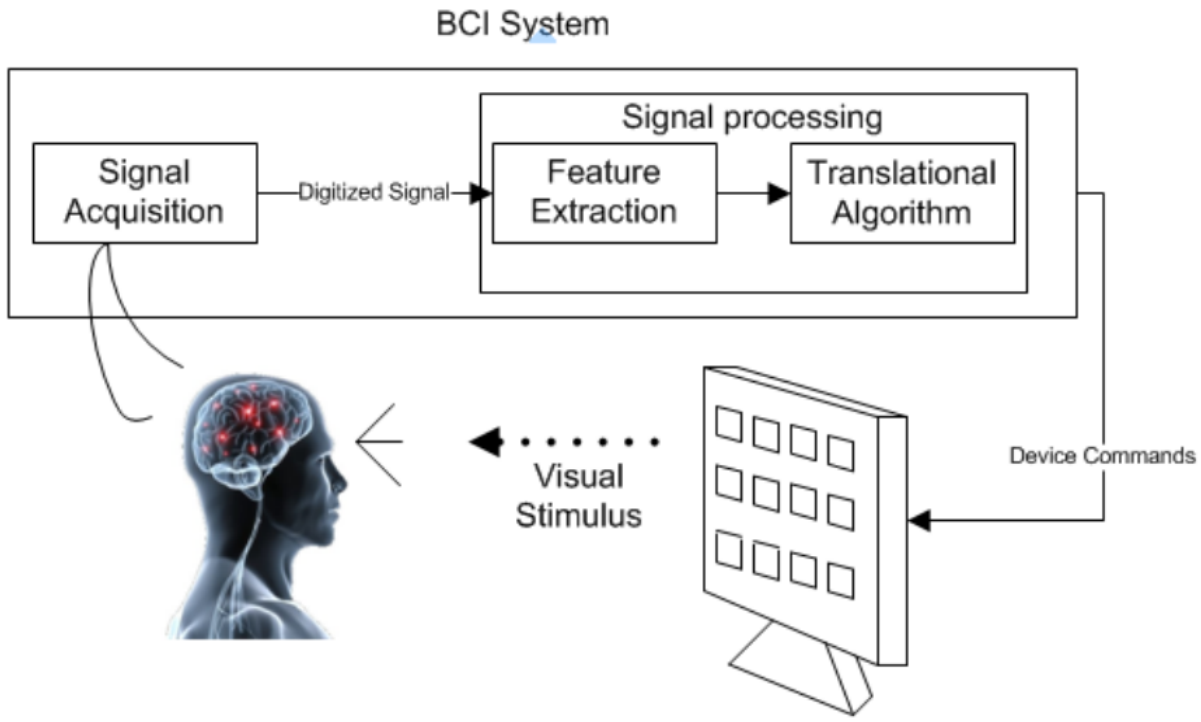

Figure 3.1: BCI block diagram

around a region of interest. The signal is then fed to the bio signal amplifier where it is pre-processed so as to improve SNR and overall signal strength. It is then digitized using a DAQ board at a predetermined frequency. The processor handles rest of the tasks involving signal processing, feature extraction, classification and decision making. Decision made governs the final action taken by an external hardware unit such as an orthosis. A feedback mechanism is supplemented to aid user in training.

3.2 SSVEP Component Estimation

The crux of our problem is to identify the user's intention by decoding the SSVEP signals emanating from the scalp with maximum accuracy and minimum time delay. Accuracy is estimated as conventionally done by finding the ratio of the misclassifications to the number of test elements. The time delay incurred in processing the signal and producing the result has two major aspects involved. Primarily, the temporal buffer size used for SSVEP signal component estimation

is responsible for substantial delay. In addition, the algorithm itself, implemented for SSVEP detection is responsible for the secondary delay incurred. Different techniques have been derived and implemented for maximizing the classification accuracy at a maximal bit rate possible. Here, bit rate refers to the number of instructions send to the implementation device per minute [6]. The classification technique discussed in the following sections mandate the need of an SSVEP EEG Source model. The source model is so defined as to replicate an ideal noise free SSVEP response. A good enough approximation as suggested by Regan et al [13] is the stimulus flicker frequency and it's harmonics, which essentially implies a low pass filter operation. Repetitive visual stimulation yields series of quasi sinusoidal TVEPs culminating into a near sinusoidal SSVEP. This model is used as a reference for further computations involved in determination of predominant SSVEP signal.

3.3 SSVEP EEG Source Model

The SSVEP EEG model used as a reference for further implementation discussions comprises of simple sinusoidal signals. In fact, this would be representative of pure SSVEP signal devoid of any noise components. The SSVEP EEG signal for N_t samples of N_y channels sampled at F_s Hertz can be represented as a sum of N_h sinusoidal harmonics of fundamental frequency f as shown below:

$$y_i(t) = \sum_{k=1}^{N_h} a_{ik} sin(2\pi k f t) \tag{3.1}$$

where i ϵ[1,2,... N_y] and t ϵ [0,1/F_s,2/F_s, . . . N_t]

In matrix form, it can be written as

$$Y = XA \tag{3.2}$$

where X = [sin(2πft) sin(4πft) . . . sin(2$N_h\pi$ft)]

$$X = [x_1 x_2 ... x_{N_h}] \tag{3.3}$$

$$A = [a_1 a_2 ... a_{N_h}] \tag{3.4}$$

We can estimate the coefficient matrix A by the method of least square error.

In order to minimize $||Y - AX||^2$, we take the derivative and equate to zero as follows,

$$\frac{d}{dA}[(Y - AX)^T (Y - AX)] = 0 \tag{3.5}$$

$$\frac{d}{dA}[Y^T Y - Y^T XA - A^T X^T Y + A^T X^T XA] = 0 \tag{3.6}$$

$$-2X^T Y + 2X^T XA = 0 \tag{3.7}$$

$$A = (X^T X)^{-1} X^T Y \tag{3.8}$$

Estimate of signal component in Y, $\hat{Y} = X(X^T X)^{-1} X^T Y$

Here, X represents SSVEP sinusoidal and their harmonics and A is the coefficient matrix of the respective sinusoidal basis. Equation 3.8 provides an intuitive understanding of the components inherently present in the channel data Y. The elements of the projection coefficient matrix A corresponds to the projection values of the channel data Y_1 , Y_2 , $...Y_{N_y}$ onto the sinusoidal basis components X_1 , X_2 , $...X_{N_h}$. In fact, as later discussed, the projection coefficient matrix A can itself be used to estimate the dominant SSVEP component. On careful analysis, it can be shown that the projection values are nothing but twice the signal power content at the respective basis frequency.

Equation 3.1 assumes zero phase shift of the basis frequencies. However, in actual recordings, this is highly unlikely and due regard must be given to the phase aspect of the signal. For this, we try two different alternatives. Firstly we extend the basis vector matrix X to include the cosine counterparts of the sinusoidal components. The new matrix X, is as shown in [3.11]

$$X = [sin(2\pi ft)cos(2\pi ft)sin(4\pi ft)cos(2\pi ft)...sin(2N_h\pi ft)cos(2N_h\pi ft)] \quad (3.9)$$

Also, it is interesting to note that the use of different permutations in X does not affect the end outcome. A permutation matrix is used when there is a need to interchange rows \ columns of a matrix. Apparently, the inclusion of Permutation matrix Π does not affect the subsequent operations performed. For column permutations on X, we post multiply by Π

Let Z = X Π, where Π is the permutation matrix. Let $\hat{Y_1} = X(X^TX)^{-1}X^TY$, $\hat{Y_2} = Z(Z^TZ)^{-1}Z^TY$.

$$\hat{Y_2} = X\,\Pi((X\,\Pi)^T(X\,\Pi))^{-1}(X\,\Pi)^TY \quad (3.10)$$

$$\hat{Y_2} = X\,\Pi(\Pi^TX^TX\,\Pi)^{-1}\Pi^TX^TY \quad (3.11)$$

$$\hat{Y_2} = X(X^TX)^{-1}X^TY \quad (3.12)$$

$$since\ \Pi^T\Pi = \Pi\,\Pi^T = I \quad (3.13)$$

$$\therefore \hat{Y_2} = \hat{Y_1} \quad (3.14)$$

Hence the inclusion of a permutation matrix does not change the operations. It proves that the specific order of arrangement of basis vectors in X is insignificant with regards to the final result.

3.4 Visual Stimulus

There is no universally accepted consensus on the nature of the SSVEP dynamics and cortical regions involved as surmised by the varying theories found in literature. SSVEPs have been hypothesized to be caused by a resonance phenomenon occurring in localized cortical sources [36]. Alternatively, another theory suggests wave-like dynamics (standing and traveling) for the propagation of SSVEPs from

a focal point of origin in the visual cortex [37]. SSVEP components have also been reported to exhibit significant variability across subjects [38], stimulation type [39], etc.

Whilst most of the variables involved are irrepressible, the stimulation source can be refined to elicit greater SSVEP response. In the past researchers have studied on the effect of stimulation color, size, intensity and the distance between user and the stimulus, etc. on SSVEP strength.

3.4.1 Effect of stimulation shapes on SSVEP response

3.4.1.1 Introduction

Effect of different shapes on SSVEP strength which was never studied before. The reason for this study comes from the fact that orientation and size specific neurons have been discovered in the occipital cortex, which activate only when excited with specific patterns. Different shapes have different orientation and size aspects that eventually lead to activation of different neuronal groups [40]. Further, neurons selectively sensitive to the orientation and size of retinal images have been observed [41]. This motivated us to believe that different shapes, which possess dissimilar orientation and size facets are likely to yield varying magnitudes of SSVEP response. Hence, we made an attempt to investigate the SSVEP response during stimulation with different shapes and their combinations. Apart from aiding in improved stimulator design for a BCI system, the study could also offer greater insight into SSVEP dynamics.

3.4.1.2 Methodology

Electroencephalogram (EEG) signals were recorded from 4 male and 1 female subjects between 22-28 years old having normal or corrected-to-normal vision. Recordings were made from scalp sites O_Z, O_1,O_2,PO_Z,PO_3,PO_4,PO_5,PO_6 as per the extended 10-20 convention. Data was acquired at a sampling frequency of

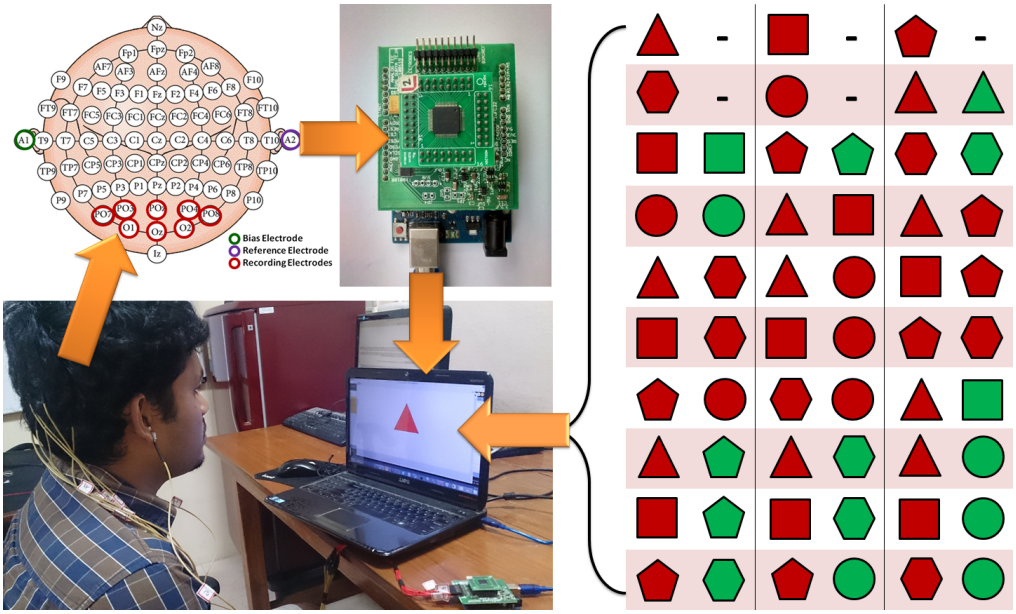

Figure 3.2: Experiment to understand the effects of different shape stimulus on SSVEP strength

250 Hz using the hardware described in chapter 2. For removing the power line interference artifacts, the data was notch filtered at 50 Hz. The stimulation was presented on an LCD monitor with a refresh rate of 60 Hz, with the stimulation paradigm consisting of different shape combinations. For simplicity in nomenclature, B denotes blank, prefixes R & G denote the colors red & green respectively and postfixes T, S, P, H & C denote the shapes triangle, square, pentagon, hexagon & circle respectively. All the shapes used for stimulation were regular polygons inscribed in a circle of radius 180 pixels. The paradigm was presented with a flicker frequency of 12 Hz (Flash frequency for single graphic stimuli and Pattern reversal frequency for pattern reversal stimuli). A single session of a subject consisted of presenting each of combinations for a period of 10s with intermittent 5s blank screen for subject relaxation. Offline analysis using 5 sessions recorded from each subject was done in MATLAB.

3.4.1.3 Signal Detection

As mentioned in section 3, we first build the source model X. Using X, we segregate the EEG data Y into signal component $\hat{Y}$ and noise component $\tilde{Y}$ by projection

theorem as:

$$\hat{Y} = X(X^T X)^{-1} X^T Y,\ \tilde{Y} = Y - \hat{Y} \tag{3.15}$$

Using the signal component $\hat{Y}$ and noise component $\tilde{Y}$, the Signal to Noise Ratio (SNR) 'p' can be computed as

$$p = \frac{Tr(\hat{Y}^T \hat{Y})}{Tr(\tilde{Y}^T \tilde{Y})} \tag{3.16}$$

The SNR 'p' that is computed for each EEG recording Y corresponding to a particular stimulation paradigm is eventually compared to identify the best shape combinations.

3.4.1.4 Results and Discussion

We observed SSVEP responses spanning the first subharmonic (6 Hz), fundamental frequency (12 Hz) and first harmonic (24 Hz) in our recordings. Shape reversal stimuli with dissimilar shapes can be literally considered to be the combination of pattern reversal stimulus of 12 Hz in the overlapping region and flash stimulus of 6 Hz in the non overlapping regions. This augmented paradigm could possibly explain the sub-harmonic frequencies seen in some of the SSVEP responses.

The subject-wise SNR values computed for each stimulation paradigm is shown in fig 3.3. A wide inter-subject variability in the SNR range was observed, which could be attributed to the fact that SSVEP responses of subjects need not be identical [38]. As seen from fig 3.3, the single graphic stimuli yielded poorer SNR values relative to the pattern reversal stimuli for all subjects. This can be substantiated by the fact that the contrast is lower in the case of single graphic stimuli relative to the pattern reversal stimuli. Shape switching alone and color switching alone yielded better SNRs than the single graphic stimulus. However, the magnitude of SNR improvement for the above cases was found to be subject dependent. Patterns with alternating color and shape yielded the highest SNRs.

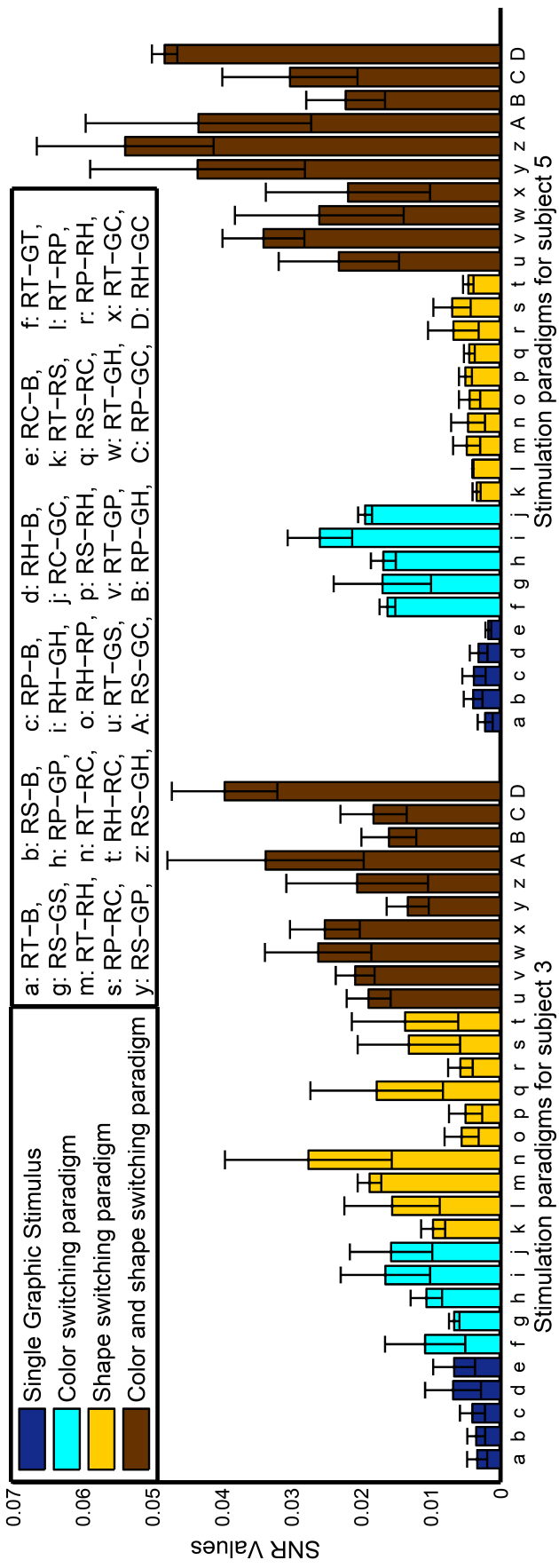

Figure 3.3: Averaged SNR values across sessions for different stimulation paradigms shown to Subjects 3 and 5. Stimulation was presented in the same order as shown along the abscissa.

Although no particular shape and color pair was observed to perform universally well, significant subject specific trends were observed. The effect of color on the SSVEPs is intuitive since they correlate directly with the stimulus contrasts. Shape effects on SNR could possibly indicate the role of the orientation and size sensitive neuronal groups of the visual cortex in the SSVEP dynamics.

Subjects reported after-image effects post stimulation on high contrast identical shape pattern reversal paradigm. For long stimulation periods, this could cause extreme user discomfort. Use of shape switching paradigm is particularly advantageous in this aspect, since it is capable of counter acting the effects of image retention after stimulation. Single graphic stimuli yielded relatively poorer SNR values relative to pattern reversal stimuli. Although no clear cut universal shape prominence was evident, a subject-specific trend was observed. Stimulation paradigms involving switching of shape and color elicited the strongest SNR values.

3.5 BCI System Design

Figure 3.4 shows an overview of the SSVEP based BCI system which was implemented as a part of this project. We used four checker stimulus with stimulation frequencies 15 Hz, 12 Hz, 10 Hz and 8.57 Hz to elicit SSVEP components in EEG. To demonstrate a BCI based assistive device, we included a toy car whose movements are controlled based on the stimulus the user is looking for an interval of time. 15 Hz , 12 Hz, 10 Hz and 8.57 Hz corresponds to forward, left, backward and right movements of the toy car respectively. We used canonical correlation analysis to classify SSVEP components.

3.5.1 Canonical Correlation Analysis

Canonical Correlation Analysis (CCA) is a multivariate statistical method to identify the underlying correlation between two data sets. CCA extends the ordinary correlation, which is constrained to a pair of variables, to include data sets of

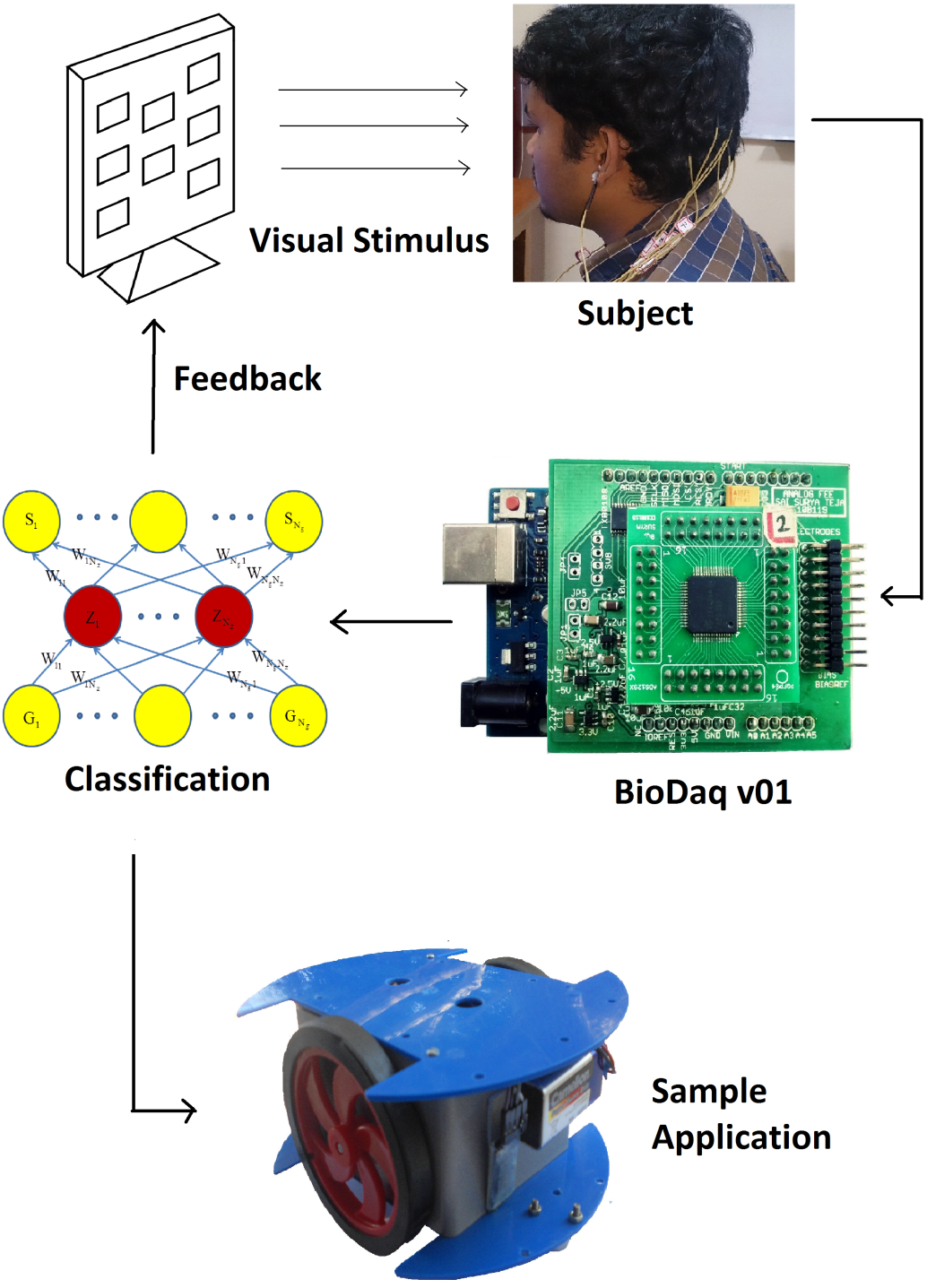

Figure 3.4: BCI system overview

variables. In CCA methodology, the correlation between canonical variables generated by linear combination of the variable data sets is studied. The coefficients used for generating the canonical variables, known as the canonical coefficients is obtained so as to maximize the correlation between the data sets.

CCA operates on two sets of variables. While one is the raw EEG data set procured from different electrodes placed across the scalp, the other is the simulated EEG base model. X of dimension $N_t \times 2N_h$ corresponds to the source model of sinusoidal. Here N_t is the number of time samples and N_h is the number of harmonics considered for the source model. The raw EEG electrode acquired data set notated as Y has a dimension of $N_t \times N_Y$, where N_t is the number of time samples as before and N_Y is the number of electrode channels. The canonical variables denoted by x and y is obtained by linear combination of canonical coefficients W_x and W_y on X and Y respectively. The canonical coefficients are obtained as a resultant of maximizing the correlation p(x,y) between x and y

$$x = X * W_x \tag{3.17}$$

$$y = Y * W_y \tag{3.18}$$

$$p(x, y) = \frac{E[x^T y]}{\sqrt{E[x^T x]E[y^T y]}} \tag{3.19}$$

$$p(x, y) = \frac{W_x^T C_{xy} W_y}{\sqrt{W_x^T C_{xx} W_x W_y^T C_{yy} W_y}} \tag{3.20}$$

To obtain the optimal canonical coefficients, we maximize the correlation coefficient p(x,y)

$$\frac{d}{dW_x} p(x, y) = 0 \tag{3.21}$$

$$\frac{d}{dW_y} p(x, y) = 0 \tag{3.22}$$

On solving, we get

$$C_{xx}W_y = p\lambda_x C_{xx}W_x \tag{3.23}$$

$$C_{yy}W_x = p\lambda_y C_{yy}W_y \tag{3.24}$$

$$where,\ \lambda_x = \lambda_y^{-1} = \sqrt{\frac{W_y^T C_{yy} W_y}{W_x^T C_{xx} W_x}} \tag{3.25}$$

Substituting and solving, we get

$$W_y = p\lambda_x C_{xy}^{-1} C_{xx} W_x \tag{3.26}$$

$$W_x = p\lambda_y C_{yx}^{-1} C_{yy} W_y \tag{3.27}$$

$$\implies C_{yy}^{-1} C_{yx} C_{xx}^{-1} C_{xy} W_y = p^2 W_y \tag{3.28}$$

$$and\, C_{xx}^{-1} C_{xy} C_{yy}^{-1} C_{yx} W_x = p^2 W_x \tag{3.29}$$

By Eigen analysis, the solution for W_x and W_y can be obtained as the Eigen vectors. Also the correlation coefficient between the canonical variables is equivalent to the square root of the eigen values. We only consider the pair of the eigen vector filters corresponding to the highest eigen value (correlation coefficient). The correlation coefficient is computed for each frequency class model and the class yielding the highest correlation coefficient value is decided as the final choice.

3.5.2 Calibration

Calibration is an essential step in SSEVP based BCI systems as the classification parameters differ from individuals and environmental conditions. In the calibration session raw EEG is acquired from 8 electrodes placed primarily around the occipital region at a rate of 256 samples per second. Specifically, the electrode sites as per the 10-20 system of EEG electrode configuration areO_Z, O_1,O_2,PO_Z,PO_3,PO_4,PO_5 ,PO_6. In this session, the subject is shown four checker patterns with pattern reversal rates of 15 Hz, 12 Hz, 10 Hz and 8.75 Hz. As per the voice commands, the

user is asked to focus on a particular stimulus. Raw EEG is stored during this interval with a frequency stamp corresponding to the stimulus. This frequency stamp is used to evaluate classification performance by varying other parameters like buffer length , correlation threshold, etc which are discussed in section 3.5.3.

3.5.3 Offline analysis

Canonical Correlation Analysis (CCA) was implemented on raw EEG calibration data. CCA was implemented on overlapping time segments of overlap period N_t /4 , whereN_t is 256 samples.The source model was constructed for all the four frequency classes namely 15 Hz, 12 Hz, 10 Hz and 8.57 Hz with inclusion up to the third order harmonic content.

Initially the source model is generated for all the four frequency classes. As discussed previously, Eigen analysis is performed to compute the canonical coefficients and correlation coefficients for each buffer length of data with respect to the generated source models. Final classification is performed by assigning the buffered time chunk of EEG data to the class yielding maximum correlation coefficient. Classification performance can be evaluated by comparing the results of CCA with the prefixed classes in calibration data at any given time. A sample plot of buffer size vs classification performance obtained for a subject is as shown in fig 3.5. A sample plot of classification % accuracy vs correlation threshold value for background obtained for a subject is shown in fig 3.6.

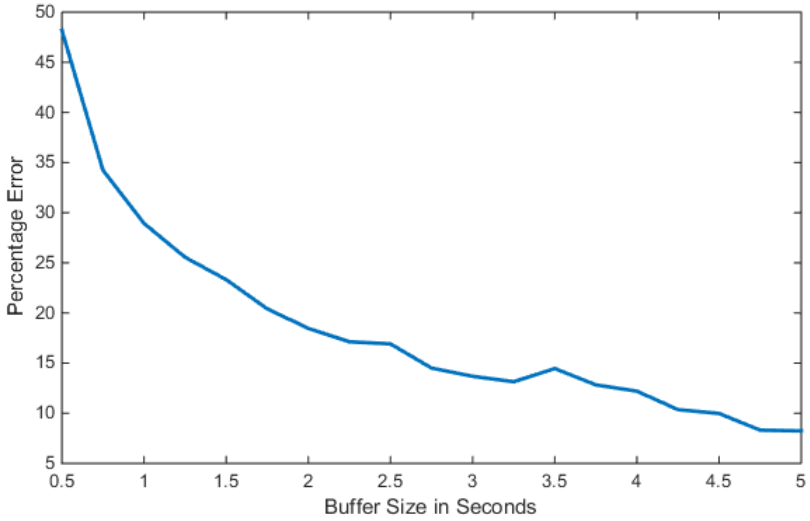

Figure 3.5: Buffer length vs classification error

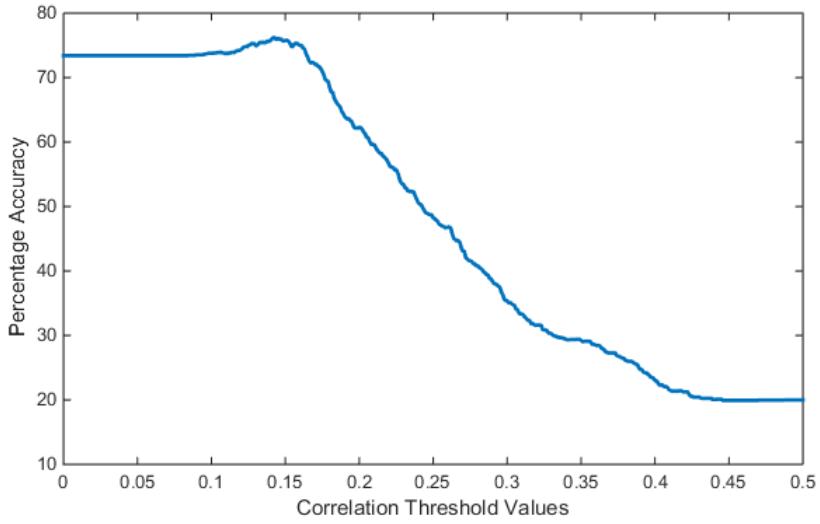

Figure 3.6: Classification % accuracy vs Correlation threshold for background

3.5.4 Online implementation

From the offline analysis, we can estimate the least buffer length for which a good classification performance can be achieved. CCA is applied on this buffer length to calculate correlation values for each frequency class. Maximum correlation value obtained from all the classes is compared against correlation threshold for the background class (obtained from offline analysis). A command corresponding to

maximum correlation class is executed only if the value is above this threshold. Otherwise, it is declared as zero class which means the user is not looking at the visual stimuli. Buffer length and correlation threshold for background class varies with the subject and other conditions like the size, intensity of the stimulus, etc. Hence, calibration is essential for this BCI system. First prize was awarded for live demonstration of SSVEP based BCI system in SHAASTRA Research Expo at IIT Madras.

Chapter 4

EOG Based HCI system

4.1 Introduction

Electrooculograms (EOGs) are strong bio-potentials induced by eye movements. The metabolically active retinal epithelium generates the Corneal Retinal Potential (CRP), which imparts the eyeball it's dipole characteristics [26]. Using bi-channel acquisition with electrodes aligned along the horizontal and vertical axes, signals pertaining to the eyeball movement can be acquired. Useful EOG features are generally observed in the 10-100 µV magnitude range and 0- 10 Hz frequency range [26]. EOGs being essentially eye movement dependent can be manipulated by a human, which offers a way for an effective human-computer interaction. Potential applications of EOG include context recognition systems [27] and assistive technology such as wheelchairs [28], alarm systems [26] etc. In this work, an EOG based virtual keyboard, a potential assistive device to aid communication for paralyzed and disabled patients with intact and functional ocular system is proposed and implemented. Despite it's relatively high magnitudes, EOG signals are still susceptible to non deterministic variations since they are governed by numerous parameters such as eye blinks, electrode placement, head movement, luminance etc., which need not be constant across subjects and sessions. To overcome these constraints, we use a simple multi-thresholding algorithm for EOG detection and classification. Prior to device use each time, threshold values are derived from a calibration session for individual subjects. After verifying the offline accuracy, the algorithm is ported to an asynchronous mode EOG based virtual keyboard. The asynchronous mode accuracy and speed is estimated to determine the efficacy of the designed system.

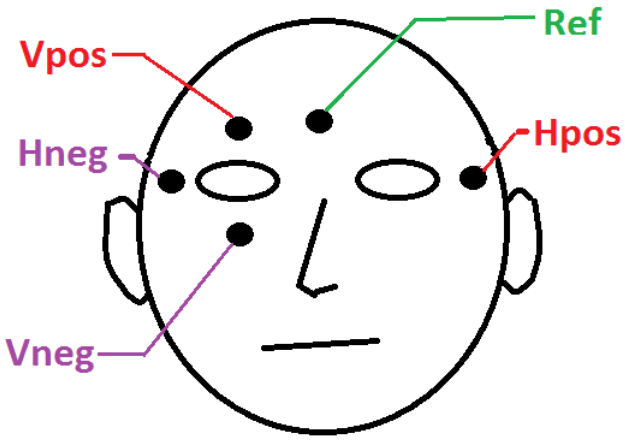

Figure 4.1: Electrode configuration to acquire EOG signals

4.2 Acquiring EOG signals

EOG is acquired by bioDaq v02 from particular positions on the face as shown in fig 4.1. Differential voltage between Vpos and Vneg corresponds to the vertical channel, which yields information about blink and vertical movement of the eyeball. Similarly, the differential voltage between Hpos and Hneg corresponds to the horizontal channel, which gives information about horizontal movement of the eyeball. A wearable mask with thin copper plates (dry electrodes) attached at specific positions as shown in fig 4.2 is designed for acquiring EOG. Both horizontal and vertical channels are sampled and digitized at a rate of 250 Hz using bioDaq v02. The digitized data is streamed continuously to PC via bluetooth for gesture classification. On the receiver side (i.e. PC), Processing (language) based applet is designed to acquire, filter (passband 0.1-30 Hz) and classify the data into commands and send to a Virtual Keyboard applet.

Figure 4.2: Wearable EOG mask with dry electrodes. U1 :

Figure 4.3: AsKey home page

4.3 EOG based assistive application - AsKey

'Processing (language)' based application is designed to implement EOG based assistive application. We call this application as 'AsKey (Assistive keyboard)'. 'Processing' IDE helps to port this application to Windows / UNIX/ MAC. Figure 4.3 shows the home page of AsKey. In this page, the user need to give details like COM port to which bioDaq v02 is connected , baud rate at which the bluetooth transmits, calibration write file name and calibration read file name. It has two buttons in the bottom viz., CALIBRATE and KEYBOARD. Respective applications will be instantiated on clicking these buttons. Details of these child applications are explained in sections 4.3.1, 4.3.2 . Any run-time errors caused due to invalid inputs by the user will be displayed in the bottom most line of the home page.

4.3.1 Calibration session

From the experiments conducted, we realized that EOG signal characteristics like amplitude and signal width slightly vary with a person to person. Hence, training

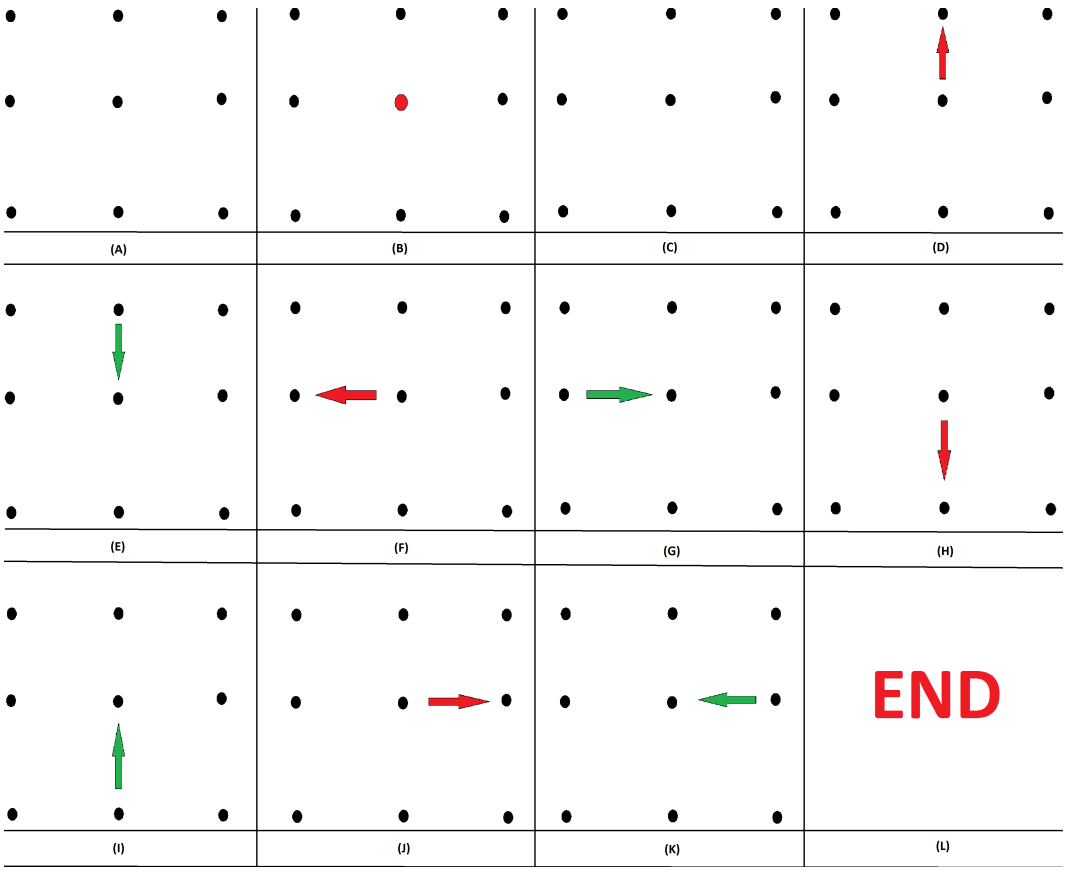

Figure 4.4: EOG calibration pictures: (A) Start, (B) Blink, (C) Relax, (D) Center -> top, (E) Top -> center, (F) Centre -> left, (G) Left -> centre, (H) Centre -> bottom, (I) Bottom -> centre, (J) Centre -> right, (K) Right -> centre, (L) End of calibration

the algorithm to understand the user EOG signals before entering into online mode was essential to achieve higher accuracy in classifying the signals.

The fig 4.4 shows the list of pictures used in calibration session. Each picture shown to the user in the full-screen mode. The user is made to sit in a fixed position at a distance of 60 cm from the monitor with his eye level at the center of the screen and asked not to turn his/her head in the training mode. He/she has to follow the audio commands sent from the software like 'blink' (B), 'up' (U), 'left' (L), 'down' (D), 'right' (R), 'center' (C). For every command from the set {B, U, L, D, R}, 'center' command was given after 2 sec. EOG signals from the two channels are acquired during this 2 sec window and stored in calibration write file (specified by the use in home page) for calculating the classification parameters. The user is requested not to perform any other eye movement other than the moving the eyeball from center to a particular position on the screen as per the audio command in this 2 sec window. After the 'center' command is given, a 'rest' period of 3 sec window is given to the user before giving the next command. EOG signals are not captured during this window. For every 'rest' command, the user is asked to look at the center and relax till he receives the next command. We followed the following order of commands in the training mode:– B-C-rest- B-C-rest- B-C-rest-U-C-rest- U-C-rest- U-C-rest-L-C-rest- L-C-rest- L-C-rest-D-C-rest- D-C-rest- D-C-rest-R-C-rest- R-C-rest- R-C-rest.

4.3.2 Keyboard

4.3.2.1 Controlling keyboard

Figure 4.6 shows a virtual keyboard, which can be controlled by eye movements. Blink, left and right movements of the eye are used to navigate and select the characters on the keyboard. This virtual keyboard is designed in 'Processing (language)' environment and can help the user to type a text using his eye movements. In this application, there is a highlighter scrolling vertically from cell to cell at

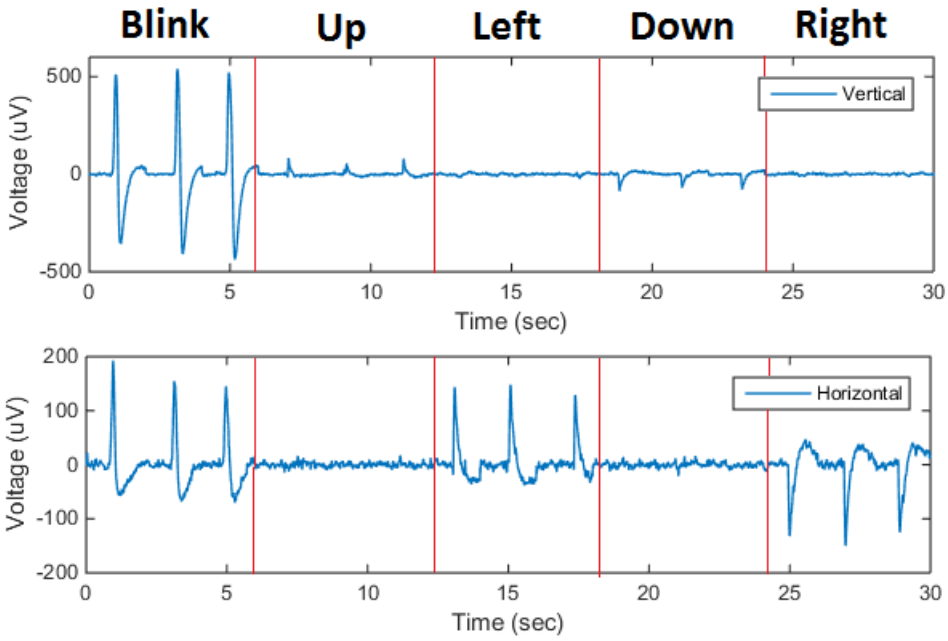

Figure 4.5: EOG signals acquired during calibration session

a speed of 1 cell/sec (speed can be adjusted according to the experience of the user) . The user needs to blink when a particular character of his/her choice is highlighted . The user needs to quickly gaze left/right outside the dimensions of the monitor and return center to move the highlighter to the left/right column respectively.

4.3.2.2 Feature extraction and Classification

As soon as the keyboard application is launched, it loads the calibration data from calibration read file as mentioned by the user in home page. The following classification parameters are calculated from the calibration data.

- B_{th} = a * maximum positive voltage in vertical channel when the user blinks
- L_{th} = b * maximum positive voltage in horizontal channel when the user gazes left.
- R_{th} = c * maximum negative voltage in horizontal channel when the user gazes right.

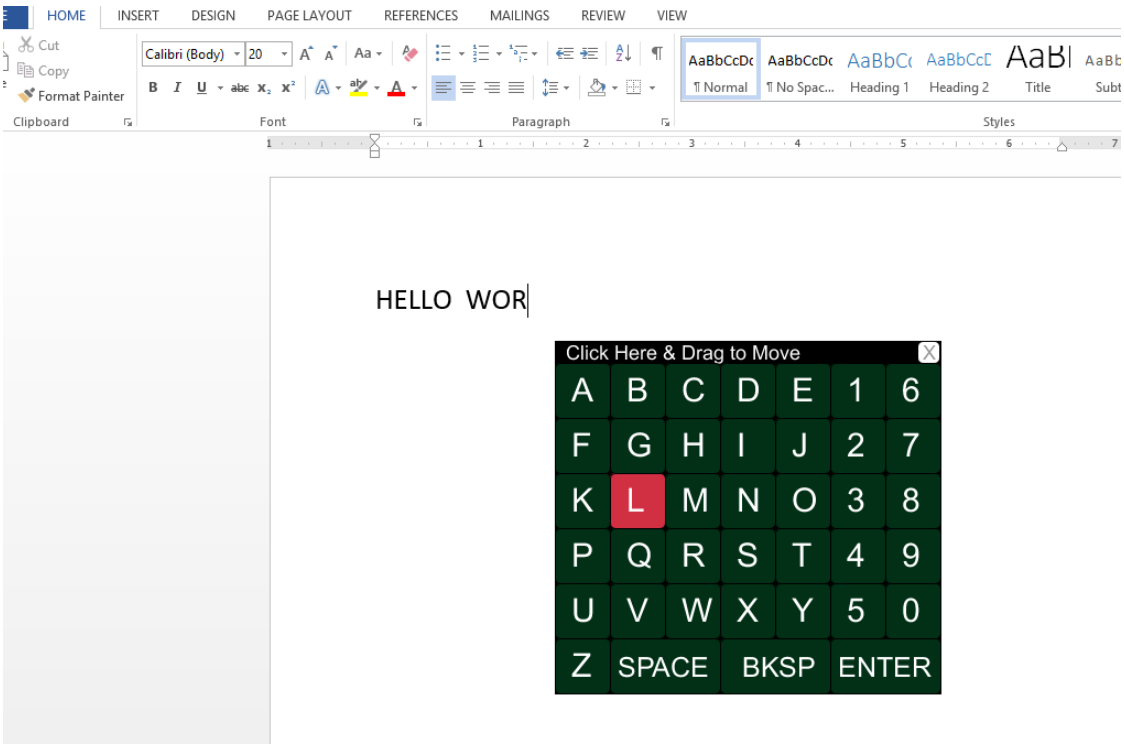

Figure 4.6: Virtual Keyboard controlled by eye movements

Here, the values of the coefficients are empirically chosen as a=0.8, b=0.9 and c = 0.9 after careful offline analysis on many calibration files. Though the calibration includes up and down movements, information related to this is not used in the keyboard application.

For every 0.2 sec (equivalent to 50 samples for a 250 Hz data rate) temporary buffer in the application is updated with the incoming 2 channel EOG data from the micro-controller after applying a passband filter of frequency ranging from 0.1 to 30 Hz. Maximum voltage in vertical channel V_{max}, the maximum and minimum voltages in horizontal channel H_{max} and H_{min} of this buffer are computed . V_{max} is then compared with B_{th} for blink detection . The current character highlighted on the keyboard is written on the text document if V_{max} is greater than B_{th} . Otherwise, H_{max} and H_{min} are compared with L_{th} and R_{th} to identify whether it is left or right movement of eye .If $H_{max} > L_{th}$, current buffer is decoded to index 1. If $H_{min} < R_{th}$, current buffer is decoded to index 2. Current buffer is decoded to index 0 if both the condition fails. As seen from fig 4.7, gesture (A) and (B) differ from transition of index from 1 to 2 or 2 to 1. A transition from 1 to 2 is

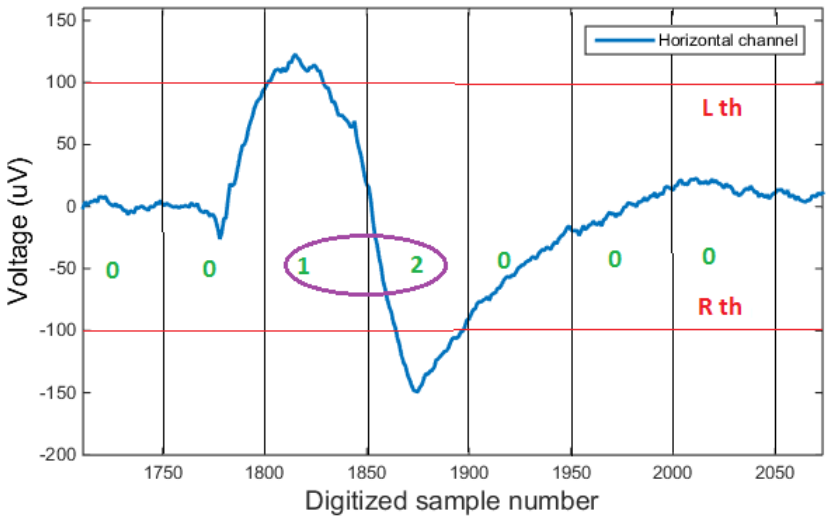

Figure 4.7: Eye movements. (A) Center -> Left -> Center , (B) Center -> Right -> Center

deciphered as left command and a transition from 2 to 1 is deciphered as right command and the highlighter is shifted to the left or right column accordingly. This system achieved 100% accuracy online with an average speed of 1 char/5 sec.

Chapter 5

Conclusions

- Designed a low cost 8 channel (single-end / differential) biopotential data acquisition system with arduino uno as the micro-controller board interfacing with the analog front end , ADS1299
- Designed a low cost 8 channel wearable and wireless biopotential data acquisition system with a form factor of 6 x 4 sq cm. Uses ATmega328p -AU instead of arduino uno board and a bluetooth module.
- Conducted experiments to study the effects of stimulation shapes on the steady state visual evoked response.Results indicate that there might exist a subject dependent connection between the elicited SSVEP and choice of shapes for the stimulation paradigm.
- Demonstrated a 4 class online SSVEP based BCI. In this, the subject can control the movements of a toy car with his brain waves. Developed software for calibration and online sessions in 'Processing (language)'.
- Improved the design of an existing wearable dry electrode mask to acquire EOG signals.
- Developed a user-end assistive application called 'AsKey'. This is a virtual keyboard controlled by eye movements. Developed an efficient and simple algorithm to classify blink, left and right movements of eye.

Chapter 6

Future scope

- Classification speed and accuracy of SSVEP based BCI system can be improved with novel and efficient algorithms.
- Design a wearable dry electrode based BCI system which should take very less setup time. The design should also focus on user comfort.
- BioDaq v02 can be improvised to a low cost product in the market.
- Wearable EOG mask should be redesigned focusing at user comfort.
- 'AsKey' application can be developed in android environment. This makes the user to carry a tablet rather than a PC along with him.
- EOG classification algorithm can be implemented in a micro-controller as it involves a basic voltage thresholding. The micro-controller can transmit only gestures rather than the complete raw data. As it transmits only few bytes, power consumption by the bluetooth module reduces to a greater extent.

List of papers submitted based on this thesis

1. Sharat S. Embrandiri , S. Sai Surya Teja , Ramasubba Reddy M., Nitin Chandrachoodan, "Effect of stimulation shapes on the Steady-State Visual-Evoked Response." In Northeast Bioengineering Conference (NEBEC), 2015 41st Annual, IEEE, 2015. (Accepted)

2. S. Sai Surya Teja, Sharat S. Embrandiri , Nitin Chandrachoodan, Ramasubba Reddy M., "EOG based Virtual Keyboard." In Northeast Bioengineering Conference (NEBEC), 2015 41st Annual, IEEE, 2015. (Accepted)

References

[1] Wikipedia. Comparison of consumer brain computer interfaces — wikipedia, the free encyclopedia, 2015. [Online; accessed 05- May-2015].

[2] Texas Instruments. Low-Noise, 8-Channel, 24-Bit Analog Front-End for Biopotential Measurements. Internet: http://www.ti.com/lit/ds/symlink/ads1299.pdf, 2012.

[3] Chris Salem and Shumin Zhai. An isometric tongue pointing device. In *Proceedings of the ACM SIGCHI Conference on Human factors in computing systems*, pages 538–539. ACM, 1997.

[4] Soochan Kim, Minje Park, Sasiporn Anumas, and Jaeha Yoo. Head mouse system based on gyro-and opto-sensors. In *Biomedical Engineering and Informatics (BMEI), 2010 3rd International Conference on*, volume 4, pages 1503–1506. IEEE, 2010.

[5] Hans Berger. On the electroencephalogram of man. sixth report. *Electroencephalography and clinical neurophysiology*, pages Suppl–28, 1969.

[6] Jonathan R Wolpaw, Niels Birbaumer, William J Heetderks, Dennis J McFarland, P Hunter Peckham, Gerwin Schalk, Emanuel Donchin, Louis A Quatrano, Charles J Robinson, Theresa M Vaughan, et al. Brain-computer interface technology: a review of the first international meeting. *IEEE transactions on rehabilitation engineering*, 8(2):164–173, 2000.

[7] Ole Jensen, Ali Bahramisharif, Robert Oostenveld, Stefan Klanke, Avgis Hadjipapas, Yuka O Okazaki, and Marcel AJ van Gerven. Using brain–computer interfaces and brain-state dependent stimulation as tools in cognitive neuroscience. *Frontiers in psychology*, 2:100, 2011.

[8] Luis Fernando Nicolas-Alonso and Jaime Gomez-Gil. Brain computer interfaces, a review. *Sensors*, 12(2):1211–1279, 2012.

[9] Niels Birbaumer, Nimr Ghanayim, Thilo Hinterberger, Iver Iversen, Boris Kotchoubey, Andrea Kübler, Juri Perelmouter, Edward Taub, and Herta Flor. A spelling device for the paralysed. *Nature*, 398(6725):297–298, 1999.

[10] Daniel S Ruchkin, Samuel Sutton, Mitchell L Kietzman, and Kenneth Silver. Slow wave and p300 in signal detection. *Electroencephalography and Clinical Neurophysiology*, 50(1):35–47, 1980.

[11] Andrea Finke, Alexander Lenhardt, and Helge Ritter. The mindgame: a p300-based brain–computer interface game. *Neural Networks*, 22(9):1329–1333, 2009.

[12] Luca Citi, Riccardo Poli, Caterina Cinel, and Francisco Sepulveda. P300-based bci mouse with genetically-optimized analogue control. *Neural Systems and Rehabilitation Engineering, IEEE Transactions on*, 16(1):51–61, 2008.

[13] D Reagan. Human brain electrophysiology. *Evoked Potentials and Evoked Magnetic Fields in Science and Medicine, Elsevier, New York*, 1989.

[14] Gernot R Müller-Putz, Reinhold Scherer, Gert Pfurtscheller, and Rüdiger Rupp. Eeg-based neuroprosthesis control: a step towards clinical practice. *Neuroscience letters*, 382(1):169–174, 2005.

[15] Francesco Di Russo, Sabrina Pitzalis, Teresa Aprile, Grazia Spitoni, Fabiana Patria, Alessandra Stella, Donatella Spinelli, and Steven A Hillyard. Spatiotemporal analysis of the cortical sources of the steady-state visual evoked potential. *Human brain mapping*, 28(4):323–334, 2007.

[16] Ola Friman, Ivan Volosyak, and A Graser. Multiple channel detection of steady-state visual evoked potentials for brain-computer interfaces. *Biomedical Engineering, IEEE Transactions on*, 54(4):742–750, 2007.

[17] Zhonglin Lin, Changshui Zhang, Wei Wu, and Xiaorong Gao. Frequency recognition based on canonical correlation analysis for ssvep-based bcis. *Biomedical Engineering, IEEE Transactions on*, 53(12):2610–2614, 2006.

[18] Matthew Middendorf, Grant McMillan, Gloria Calhoun, Keith S Jones, et al. Brain-computer interfaces based on the steady-state visual-evoked response. *IEEE Transactions on Rehabilitation Engineering*, 8(2):211–214, 2000.

[19] Xiaorong Gao, Dingfeng Xu, Ming Cheng, and Shangkai Gao. A bci-based environmental controller for the motion-disabled. *Neural Systems and Rehabilitation Engineering, IEEE Transactions on*, 11(2):137–140, 2003.

[20] Hovagim Bakardjian, Toshihisa Tanaka, and Andrzej Cichocki. Optimization of ssvep brain responses with application to eight-command brain–computer interface. *Neuroscience letters*, 469(1):34–38, 2010.

[21] Brendan Z Allison and Jaime A Pineda. Erps evoked by different matrix sizes: implications for a brain computer interface (bci) system. *Neural Systems and Rehabilitation Engineering, IEEE Transactions on*, 11(2):110–113, 2003.

[22] Dan Zhang, Alexander Maye, Xiaorong Gao, Bo Hong, Andreas K Engel, and Shangkai Gao. An independent brain–computer interface using covert non-spatial visual selective attention. *Journal of Neural Engineering*, 7(1):016010, 2010.

[23] Gert Pfurtscheller and A Aranibar. Event-related cortical desynchronization detected by power measurements of scalp eeg. *Electroencephalography and clinical neurophysiology*, 42(6):817–826, 1977.

[24] C Neuper and G Pfurtscheller. Event-related dynamics of cortical rhythms: frequency-specific features and functional correlates. *International journal of psychophysiology*, 43(1):41–58, 2001.

[25] Ulrich Hoffmann, Jean-Marc Vesin, and Touradj Ebrahimi. Recent advances in brain-computer interfaces. In *IEEE International Workshop on Multimedia Signal Processing (MMSP07)*, number LTS-CONF-2007-063, 2007.

[26] S Venkataramanan, Pranay Prabhat, Shubhodeep Roy Choudhury, Harshal B Nemade, and JS Sahambi. Biomedical instrumentation based on electrooculogram (eog) signal processing and application to a hospital alarm system. In *Intelligent Sensing and Information Processing, 2005. Proceedings of 2005 International Conference on*, pages 535–540. IEEE, 2005.

[27] Andreas Bulling, Daniel Roggen, and Gerhard Tröster. It's in your eyes: towards context-awareness and mobile hci using wearable eog goggles. In *Proceedings of the 10th international conference on Ubiquitous computing*, pages 84–93. ACM, 2008.

[28] Rafael Barea, Luciano Boquete, Manuel Mazo, and E López. Wheelchair guidance strategies using eog. *Journal of intelligent and robotic systems*, 34(3):279–299, 2002.

[29] S Yathunanthan, LUR Chandrasena, A Umakanthan, V Vasuki, and SR Munasinghe. Controlling a wheelchair by use of eog signal. In *Information and Automation for Sustainability, 2008. ICIAFS 2008. 4th International Conference on*, pages 283–288. IEEE, 2008.

[30] Wijerupage Sardha Wijesoma, Kang Say Wee, Ong Choon Wee, Arjuna P Balasuriya, Koh Tong San, and Low Kay Soon. Eog based control of mobile assistive platforms for the severely disabled. In *Robotics and Biomimetics (ROBIO). 2005 IEEE International Conference on*, pages 490–494. IEEE, 2005.

[31] Arslan Qamar Malik and Jehanzeb Ahmad. Retina based mouse control (rbmc). *World Academy of Science, Engineering and Technology*, 31:318–322, 2007.

[32] Manuel Merino, Octavio Rivera, Isabel Gómez, Alberto Molina, and Enrique Dorronzoro. A method of eog signal processing to detect the direction of eye movements. In *Sensor Device Technologies and Applications (SENSORDEVICES), 2010 First International Conference on*, pages 100–105. IEEE, 2010.

[33] Ali Bülent Usakli, Serkan Gurkan, Fabio Aloise, Giovanni Vecchiato, and Fabio Babiloni. On the use of electrooculogram for efficient human computer interfaces. *Computational intelligence and neuroscience*, 2010:1, 2010.

[34] Patterson Casmir D Mello and Sandra D Souza. Design and development of a virtual instrument for bio-signal acquisition and processing using labview. *Int. J. Adv. Res. Electr. Electron. Instrum. Eng*, 1(1):1–9, 2012.

[35] Divya Swami Nathan, A Prasad Vinod, and Kavitha P Thomas. An electrooculogram based assistive communication system with improved speed and accuracy using multi-directional eye movements. In *Telecommunications and Signal Processing (TSP), 2012 35th International Conference on*, pages 554–558. IEEE, 2012.

[36] Christoph S Herrmann. Human eeg responses to 1–100 hz flicker: resonance phenomena in visual cortex and their potential correlation to cognitive phenomena. *Experimental brain research*, 137(3-4):346–353, 2001.

[37] Guy R Burkitt, Richard B Silberstein, Peter J Cadusch, and Andrew W Wood. Steady-state visual evoked potentials and travelling waves. *Clinical Neurophysiology*, 111(2):246–258, 2000.

[38] Rafał Kuś, Anna Duszyk, Piotr Milanowski, Maciej Łabęcki, Maria Bierzyńska, Zofia Radzikowska, Magdalena Michalska, Jarosław Żygierewicz,

Piotr Suffczyński, and Piotr Jerzy Durka. On the quantification of ssvep frequency responses in human eeg in realistic bci conditions. *PloS one*, 8(10):e77536, 2013.

[39] Danhua Zhu, Jordi Bieger, Gary Garcia Molina, and Ronald M Aarts. A survey of stimulation methods used in ssvep-based bcis. *Computational intelligence and neuroscience*, 2010:1, 2010.

[40] David H Hubel and Torsten N Wiesel. Receptive fields and functional architecture of monkey striate cortex. *The Journal of physiology*, 195(1):215–243, 1968.

[41] FW Campbell and L Maffei. Electrophysiological evidence for the existence of orientation and size detectors in the human visual system. *The Journal of Physiology*, 207(3):635–652, 1970.

Appendix A

Bill of materials

Part	Function	Quantity
0.1μF ,0.01 μF, 2.2 μF, 10 μF	Decoupling capacitors	10
1.5 nF	For band passing the bias reference signal of ADS1299	1
1 μF	Decoupling capacitors for ADS1299	15
4.7 nF , 5 KΩ	Used in anti-aliasing filters for each electrode input.	20
100 μF	Bypass capacitor for ADS1299	1
1 MΩ	For band passing the bias reference signal of ADS1299	1
10 KΩ	Pull up resistors	5
Electrodes	To acquire EEG signals	8
ADS1299	Acts as a bio-potential amplifier and digitizer	1
TPS60403	Charge pump inverter. Helps to generate AVSS	1
TPS72325	To generate AVSS (=-2.5V)	1
TPS73225	To generate AVDD (=2.5V)	1
TPS70933	To generate DVDD (=3.3V)	1
ATmega328P-AU	To interface with ADS1299 and transmit data to PC	1
HC05	Bluetooth module used in Biosig v02	1

Table A.1: Bill of materials

Appendix B

Choosing a bluetooth module for wearable assistive devices based on biopotentials

Table B.1 shows some of the bio-potential signals with different amplitude and frequency ranges. Among all biopotential signals EMG has a higher bandwidth. So, we need a sampling frequency of more than 20KHz. Table B.2 shows the data generated for 8 channels for different resolution of ADC at a sampling speed of 20KHz. All the existing Bluetooth modules in the market communicate via UART (Universal Asynchronous Receiver Transmitter) protocol. All the existing micro-controllers support this communication protocol. Table B.3 shows some of the bluetooth modules with different maximum baud rates.

Sampling speed (Hz)	ADC resolution		
	8 bits	12 bits	24 bits
500	0.030 Mbps	0.045 Mbps	0.091 Mbps
1000	0.061 Mbps	0.091 Mbps	0.183 Mbps
1500	0.091 Mbps	0.137 Mbps	0.274 Mbps
2000	0.122 Mbps	0.183 Mbps	0.366 Mbps

Table B.4: Data generated for different ADC resolution and sampling speed

Maximum current consumption (active mode) is around 30-50mA for the above bluetooth modules. They have a default firmware inbuilt in them, which enables

Biopotential signal	Amplitude(μV)	Bandwidth (Hz)
EEG	1-100	0-150
EOG	5-200	0-50
EMG	20-2000	0-10000
ECG	500-4000	0.01-250

Table B.1: Biopotential signal amplitudes and frequency ranges

ADC bit resolution	Generated Data (Mbps)
8	>0.152*8 = 1.216
12	>0.228*8 = 1.824
24	>0.457*8 = 3.656

Table B.2: Data generated for a given ADC resolution

Bluetooth module	Max baud rate (Mbps)
HC-05	1.318
RN-42	0.87
BTM410	0.87
WT12	2.63
WT32	2.63
WT32i	3.515

Table B.3: Bluetooth modules

the user to change the data rate,name, connectivity password,etc through wireless communication. Table B.4 gives an analysis of data generated for different ADC resolution and sampling speed.All the above Bluetooth modules satisfy the above sampling speeds. So, bluetooth module with low cost, low power, small size and high reliability must be selected.